CHARACTERIZATION OF MULTIAXIAL FRACTURE STRENGTH OF TRANSVERSELY ISOTROPIC AGOT GRAPHITE

by

H. ALAN HACKEROTT

B. S., Kansas State University, 1980

A MASTER'S THESIS

submitted in partial fulfillment of the

requirements for the degree

MASTER OF SCIENCE

Department of Mechanical Engineering

KANSAS STATE UNIVERSITY
Manhattan, Kansas

1982

Approved by:

George W. Eggeman
Major Professor

Characterization of Multiaxial Fracture Strength of Transversely Isotropic AGOT Graphite

H. Alan Hackerott

November, 1982

ACKNOWLEDGEMENTS

The author wishes to express his deepest gratitude to Dr. George W. Eggeman, and Dr. C. L. Huang for their guidance and patience throughout the course of this study.

Sincere appreciation is also extended to Dr. S. E. Swartz for his suggestions and participation on the supervisory committee. Special thanks is extended to Dr. H. S. Walker for generously sharing his cache of surplus salvage and to Drs. R. V. Turnquist and B. W. Jones for loaning equipment.

Indebtedness is owed to Gary Thornton for his assistance, use of facilities, and help in salvaging hydraulic hardware for fabricating the biaxial test apparatusl that made this experimental work possible. He was also responsible for the close tolerances of the machined specimens.

Also my deepest appreciation is expressed to the Department of Nuclear Engineering for providing the material tested and to various faculty in the Department of Civil Engineering for providing additional testing equipment and valuable suggestions.

Finally, appreciation is expressed to the Department of Mechanical Engineering for financial support for a portion of this study.

TABLE OF CONTENTS

CHAPTER I

INTRODUCTION

Purpose of Research and Complications

There is a general lack of good fracture data in the compression-compression quadrant of the biaxial stress space for all materials. The emphasis of these experimental investigations was to obtain additional data on biaxial compression fracture strengths for a brittle transversely isotropic material. A fabricated multiaxial testing apparatus was designed and used to approximate loadings of hollow cylinders in biaxial stress space. Uniaxial tension and compression tests were also performed. The state of biaxial compression can be approximated by applying an axial compressive load and an external pressure to a cylinder which is specifically designed for the purpose of obtaining the true material strength. This test requires the balancing of two conflicting requirements; namely, uniform strain field and resistance to buckling.

Major difficulties in this approach are that stresses, other than those expected, arise from axial load and applied pressure. A complication also arises in the complex geometries of a test cylinder, when a particular load thought to be uniaxial creates a multiaxial stress state. This can alter the apparent strength since most material behavior and theories predict a change in strength for multiaxial loadings. Buckling load determinations are also complicated and inexact.

Factors such as end conditions, geometry, and dimensional tolerances can cause the buckling loads to differ widely from the calculated values. In addition, the load-carrying capability or strength of a material is dependent upon many other variables such as the application of forces, temperature, corrosion, and radiation.

Problems in Evaluating Load-Carrying Capabilities

A common philosophy of all strength of material theories is to predict the behavior of a material in a generally complex stress state based on simple criteria like uniaxial strength tests. All strength theories, whether based on a mechanistic or emperical approach, need verification by experiment.

To evaluate the load carrying capability in the design of a structure, it is necessary to predict both yielding and brittle fracture. Mathematical models used to evaluate this are referred to as strength criteria. Largely emperical, these criteria are functions of applied stresses or strains. All of these criteria can be expressed, at least piece-wise, as:

$$f(\sigma_k) = 1, \; k = 1,\ldots,6,$$

where σ_k is the contracted notation of the stress tensor. A stress state not enclosed by the hyperspace as defined by this equation in six-dimensional stress space implies fracture or plastic yielding. Plastic yielding and brittle fracture are different phenomena and involve different material mechanics. However, yield criteria can be

applied to the fracture of materials because brittle fracture is thought to be preceded by incipient plastic yielding.

Testing the strength of a material involves some method that requires knowledge of the applied stresses and the evaluation of the material response. The testing of brittle materials that may fail by rapid crack propagation because of local failure, presumably tensile, originating from even a minor stress concentration is complicated and difficult. Brittle materials, unlike ductile materials, exhibit plastic yielding before fracture. Any stress concentration due to geometry, end conditions, or load applications may also initiate a total failure.

Material behavior under multiaxial loading is, in general, not the same as for the uniaxial case. Under multiaxial loadings, significant increases or decreases in material strength can be exhibited. More adequate characterization of material behavior is needed for general multidimensional loadings. Strength criteria are a function of stress (or strain) that, if satisfied, imply failure. It is desirable to have this function operationally simple as well as accurately descriptive. No single criterion based on a failure mechanism is likely to describe a particular material, which is not surprising, considering the diversity of failure mechanisms that can be displayed by a material. An accurate characterization of a material by the use of a minimum number of tests is also desired. Better methods of analysis attributed largely to imporoved computer techniques facilitate the analysis of material stress. Correspondingly better knowledge of material properties is needed to better utilize the improved analytical procedures now available.

Characteristics of Graphite

Graphite is a nonlinear material, and the current trend is to use nonlinear constitutive relations to better model its behavior. Its properties differ for each of the three mutually perpendicular material axes oriented along the extruded axis. Most materials exhibit some degree of anisotrophy. Rolled steel, for example, has an orthotropic crystal orientation, but this aspect is usually neglected in strength analyses as it complicates the constitutive relationships. For a material to be transversely isotropic, the material properties in a plane containing two material principal axes are considered invariant.

Many grades of graphite are readily available and they have properties that make them useful for special applications. Graphite has a relatively high thermal conductivity, low thermal expansion coefficient, high resistance to thermal shock, high melting point, and resistance to chemical erosion. In nuclear applications, it is used as a neutron reflector and in reactor core structures. It is also used for re-entry protection for space vehicles as well as arc furnaces and rocket nozzle throats.

Graphite is considered to be a brittle material; i.e., it exhibits limited crystalline slip or plastic deformation. However, like most brittle materials, it can exhibit plastic flow under multiaxial compression. Other characteristics of graphite that in some ways complicate modeling of its behavior are nonlinear and nonconservative stress-strain relations, transverse isotropy, nonhomogeneity and a change in volume under uniaxial stress. The Bauschinger effect, i.e., compression properites that are different from tension properties, is

more significant in graphite than in most materials.

Objectives

The specific objectives of this study were to: (a) characterize fracture tests of EGCR-type grade-AGOT graphite by the application of a strength tensor theory, and (b) design and fabricate a test apparatus to improve the acceptability of the pressure-vessel method for the biaxial-compression test.

CHAPTER II

LITERATURE REVIEW

Introduction

Many theories of strength of materials have been proposed during the last one hundred years. Some are emperical while others are based on micro-mechanisms of fracture. Despite a formal similarity between yield conditions and fracture conditions, the underlying physical phenomena are fundamentally different. A fracture criterion predicts failure that is preceded by negligible inelastic deformation that characterizes brittle materials. Other characteristics of brittle materials that complicate testing and evaluating material behavior include differing tensile and compressive strengths, appreciable size effects, and high scatter of data.

This review is concerned with theories, test procedures, and results dealing with a brittle antisotropic material; namely, EGCR-type AGOT graphite. Of interest and pertinance to this topic are methods of testing and evaluating metallic materials, concrete, and rocks.

Failure Theories

It was pointed out in a conference held in 1970 that the continuum aspects of graphite design had its origin at the Oak Ridge National Laboratory ten years earlier. At that time it became apparent that

available data and design methods were not adequate to assess the structural adequacy of graphite elements used for the Experimental Gas-Cooled Reactor (EGCR). A decade later Rowley [37] emphasized in the keynote address at this conference that graphite technology still lacked a practical continuum model to account for its inelastic effects. Moreover, significant parameters to define fracture criteria had not yet been formulated and few quantitative data in this area were available. The design and analysis of graphite structural components was hindered by the lack of an accurate description of graphite fracture. Sufficient data were still not available to utilize in the sophisticated computer programs that were then available for structural analysis. In a 1980 symposium, Hu, Swartz, and Huang [22] state that with the advent of complex finite element models, the thrust of problem solving in solid mechanics has shifted to more accurate material description for para-isotropic materials.

All failure theories reported in the literature can be expressed as a function of applied stress. The constants in this equation, whether based on a continuum or microscopic approach, are evaluated experimentally, preferably with simple fracture tests. There is still some controversy as to the standards for this test. An excellent review of literature concerning failure theories as they apply to graphite is presented by Tang [40]. He reviewed the failure theories and divided them into four basic groups as follows: (1) the maximum stress (strain) theory, (2) the maximum shear stress theory, (3) the maximum strain energy theory, and (4) the maximum distortion energy theory. Other names found associated with these theories are Rankine, Tresca, Beltrami, and Von Mises. There are, of course, many applications and

extensions of these theories and new ones are being continuously reported. However, considering the variability in some of the available data and the possibility of plastic buckling preceding fracture, Mair [31] and others question the need for more elaborate theories.

Tang lists seven requirements that he considers necessary or desirable for a three-dimensional failure criteria for transversely isotropic graphite. These requirements involve consideration of transversely isotropic material symmetry, the Bauschinger effect, a dependence on the mean stress, and compressability. In addition he further states that these criteria should be a scaler function capable of predicting failure for all stress states and represent a closed surface about the zero stress state. Tang concludes after the investigation of specific deficiencies for all theories applicable to graphite that an operationally simple criteria proposed by Tsai and Wu [60] meets these requirements for graphite.

Tsai and Wu's theory [43] is a strength tensor failure criterion in a tensorially invariant form with stability conditions. The most general form of this type of theory was presented by Gol'denblat and Kopnov [15]. Extensions and special cases of this theory have also been done by Priddy [36], Merkle [32], and Huang and Kirmser[23]. Expressing failure theories in tensorially invariant form makes them well suited to the characterization in three dimensions of nonisotropic materials. A list of characteristics of tensor polynomial failure theories are given in references Gol'denblat [15] and Tsai [43].

Tsi and Wu's theory is operationally simple and transformable. Other special attributes of their theory include treating interaction terms as independent components and accounting for different material

symmetries.

A proposed three-dimensional strength tensor theory of Tsai and Wu for a transversely isotropic brittle solid with a suggested test procedure can be found in Tang's investigations [40]. The three-dimensional polynomial for a transversely isotropic material is defined by:

$$F_1(\sigma_1 + \sigma_2) + F_3\sigma_3 + F_{11}(\sigma_1^2 + \sigma_2^2 + 2\sigma_6^2) + F_{33}\sigma_3^2 + F_{44}(\sigma_4^2 + \sigma_5^2) + 2F_{12}(\sigma_1\sigma_2 - \sigma_6^2) + 2F_{13}(\sigma_1\sigma_3 + \sigma_2\sigma_3) = 1 \quad (2.1)$$

This equation was written with reference to the axes or the x_1, x_2, and x_3 directions, where x_3 is the axis of material symmetry, parallel direction, or the axial direction. The x_1 and x_2 directions are in the plane perpendicular to the longitudinal material axis, the plane with invariant material properties.

Ho [20] developed test specifications for nuclear graphite for the General Atomic Company that involved graphite cylinders. In his review of experimental procedures, Tang credits Ho with providing the best and most well defined biaxial test procedure for graphite.

Uniaxial Investigations

There is no universally accepted testing technique that provides a uniform stress state to failure in a uniaxial test specimen. The ASTM and the British Standard have suggested standards for uniaxial tests and failure theories. A large number of reports are also available on the testing of ductile materials. However their application to brittle

materials is limited. Brittle materials can exhibit larger variations in strength due to variations in test techniques than ductile materials. Comparisons between uniaxial tests with differing techniques are difficult for brittle materials. The ASTM standard for compression testing of carbon and graphite has provisions for the use of different materials placed between the specimen and the end platen. According to many investigators, this can have significant influences on strength.

Peng [35] investigated solid cylinders of rock and steel under uniaxial and triaxial loading. He subjected these to the following end boundry conditions: perfect confinement, direct contact, neoprene rubber, and teflon inserts. He found that highly non-uniform stress distributions are developed under end conditions of perfect confinement. In the uniaxial case, particularly in compression, there are numerous reports on the effect of end conditions, geometries and their effect on apparent strength.

A method of tensile testing employed by Sedlacek [38] has been used by many investigators in tensile testing of brittle materials, where applicable . This method involves the application of pressure inside a short tube or ring placed between two parallel plates. When the tube geometry is symetrical, this has yielded large fracture stress values. However, this method cannot be used to determine properties for a particular direction. Swartz et. al. [39] successfully demonstrated a method for tensile testing of uniform concrete and rock cylinders that involves the use of adhesive bonding and unique alignment procedures that provide the accuracy of the standard compression testing.

Size effects are important since the growth of material flaws is considered by most investigators to be of paramount importance in brittle material fracture. As Jaganout [25] points out, graphite fibers have high strength because their cross-sectional area is small enough to minimize the probability of a crack initiating flaw.

Uniaxial investigations of graphite involve many geometries and loading methods for both tensile and compressive specimens. Greenstreet et al. [17] investigated the mechanical properties of AGOT but did not include biaxial tube tests. They did investigate uniaxial properties, area effects, cyclic, and hydrostatic loadings. Their conclusion was that size effects in tension are small or nonexistent for AGOT within the size range investigated (0.128" to 0.625" in diameter). Properties they report are based on averages of several test specimen geometries. In the direction parallel to the material's extruded axis, they report tensile and compressive strengths of 1570 psi and 4800 psi respectively. In the perpendicular material direction, they report a 930 psi tensile strength and a 4930 psi compressive strength. In Nuclear Graphite, Nightingale [34] also reported compression strength values of 6000 psi compressive for both parallel and transverse directions, as well as tensile strengths of 2400 psi and 2000 psi for the parallel and transverse directions of AGOT. They also acknowledged that variability in properties between blocks and samples within blocks should be treated on a statistical basis.

Biaxial Investigations

Much of the earlier experimental and theoretical work on cast iron was conducted by Grassi and Cornet [8], Fisher [14], Coffin [7], and Mair [31]. In the c-c quandrant, Coffin suspected that failure of his four data points to correspond to theoretical values was due to instability rather than complete separation on a particular plane. Mair, [31] working with cast iron cylinders, postulated that plastic buckling preceded fracture and that this phenomenon was responsible for scatter in his twenty data points in the c-c quadrant.

The fracture behavior of ceramic and graphite materials with varying degrees of isotrophy are limited in number and scope. Ely [9,10,11,12,13], Merkal [32], Jortner [27, 28, 29, 30], Taylor [41], Weng [45, 46], Greenstreet et al. (17), and Broutman (3,4), conducted multiaxial tests on ceramic and graphite materials. Biaxial tests have been performed on different graphite grades (Graph-I-tite-G, AXM, AXF, ATJ, and ATJ-S and AGOT). Materials other than graphite tested by similar biaxial techniques are plexiglass, boron nitrate, alumina ceramic, and magnesium silicone.

Specifically for biaxial compression, Ely [13] did tests on Graph-I-Tite uniform circular cylinders, including c-c for six L/D (Length/Diameter) ratios. Normal specimen ID (Inside Diameter) and wall thickness were 1.190" and 0.075", respectively. He considered apparent differences in strengths represented by these diffferent geometries attributable to what he calls the expansion effect. He also considered strength values in the c-c quadrant where the lateral expansion caused by the axial load is negated by the external pressure to be the only

points representative of true material strength. He designated this region the crossover zone.

Weng [45], like Ely, did c-c tests on ATJ graphite for five different gauge lengths and concluded that buckling was largely affected by specimen length. His cylinders had an ID of 0.885" and an OD of 0.985". Weng and Ely's data in the c-c quadrant, as a function of specimen length, are similar. In the lower portion of the quadrant representing uniaxial compression, specimen length decreases strength. Along a radial line in the c-c quadrant, similar fracture strengths were displayed by different gauge lengths. Above this load path, strength differences for different specimen lengths are prominent. For load paths closer to the compressive hoop strength axis, short tubes gave strengths twice as large as long tubes. Jortner [29] used several tube geometries to investigate their strengths. He used NASA's Shell Analysis Manual [2] to estimate buckling loads of compression-compression specimens to be 6000 psi axial and 3800 psi tangential. This manual involves the use of emperical and theoretical design methods for determining buckling of shells.

Tang's [40] principle conclusion for biaxial compression testing is that premature buckling causes unrepresentative failure . He did not, however, speculate that this premature buckling resulted in an apparent decrease in material strength. Tang also cites Weng's compression test program as having instability in the arch action. However, Weng [46] in his paper says nothing of this. Tang, like all other investigators involved with biaxial testing of graphite, concludes that more data and modified test procedures are needed.

Concern about stress distribution in a statically-loaded graphite

cylinder prompted Jortner [30] to apply Jones' SAAS-II-Finite element analysis [26] to find an improved specimen geometry to achieve better stress distribution. He also used a method that gave similar results based on simple geometry. Correlation of these methods revealed that the analytical method produced results closer to the recorded strain gauge data. The variation between inside and outside hoop stresses was five percent. The size effect; i.e., how the cross sectional area of the cylindrical specimen affects strength for biaxial tubes, was addressed by Ely [10, 11] and Jortner [29, 30]. Ely found that under tension loading, wall thickness of 0.06" with an ID of 1" was sufficient to represent the strength of Graph-I-Tite graphite. Jortner concluded that a 0.05" wall thickness may be insufficient represented the bulk of the material in compression-compression. However in tension loadings Jortner [20] considers a 0.05" wall thickness representative of ATJ-S graphite.

Babcock's [1] ten reported tests of ATJ-S used a cylinder wall thickness of 0.25" and an ID of 2" with a length of 5". Biaxial compression tests of five alumina ceramic cylinders of two lengths with a load path ratio of 2/1 hoop to axial stress were conducted by Broutman [3]. He used bearing plates of steel, tungston carbide, and alumina. His strength results were one-half as much as he had predicted by using Griffith's theory. Ely [12] used twelve tapered and non-tapered graphite tubes on stainless steel seats on a single load path in the lower portion of the c-c quadrant, i.e., predominantly axial loading to obtain fracture data. The tapered specimens gave larger strength results. However, he considered these results in the c-c quadrant to be unreliable because of non-uniformity in the specimen

stress field. Jortner [29] reported biaxial fracture data in the middle of the c-c quadrant for only two tapered specimens of ATJ-S graphite. His specimens were bonded to the end platens along the outside surfaces.

Ho [20] used bonded end conditions which were fixed in biaxial tests. Brittle ceramic tubes of different end condition geometries under axial compression are reported by Nadai [33]. He demonstrated increasing load-bearing capacities of tubes where geometry creates a biaxial stress field from uniaxial loading.

Jortner [30], concluded that surface finish does not affect strength as much as predicted. By using Griffith's [18] criteria applied to spherical surface flaws he also found that visible surface flaws apparently do not coincide with the origin of fracture. Ely [10] also examined each specimen for visible surface defects and similarly concluded that there was no correlation between surface flaws and origin of fractures.

Additional data sought by researchers in biaxial tests of graphite include the effects of elevated temperatures and the effects with different histories of applied irradiation, thermal, and mechanical stress (Taylor [41], Babcock et al. [1] and Greenstreet et al. [17]). All investigators report an increase in material fracture strength with elevated temperatures or irradiation.

Testing Apparatus

Multiaxial test machines involve many principles of obtaining the desired stress field. The method of loading a cube perpendicular to

its faces involves great difficulties in determining materials strain response, particularly for brittle materials requiring uniform force application on the material face. Other test methods that have been employed for multiaxial testing include the use of solid and hollow tubes, the Brazilian test, and membrane tests.

The biaxial test apparatus used in the study of the behavior of hollow tubes of graphite involves several designs. One type of test method used is the application of an external force usually from a standard test machine to create axial load. The pressure applied to the inside or outside of the biaxial tube is generated by an external source or by pistons subjected to this same axial force. This method provides a constant ratio of axial load to apply pressure. A similar method used only for axial tension and hoop compression was employed by Broutman [4]. His method involves interchangeable pistons and sleeves to provide different axial loads for different bushings and thus different load paths.

Jortner [29] reported pore pressure can affect the fracture of a porous brittle material like ATJ graphite by causing localized tensile failure. Jortner considered this to be significant at pressures above 1000 psi.

Various barriers were used on several types of graphite in different test programs to prevent localized pore pressure effects. Jortner [29] used florasilicone rubber manufactured by Dow Corning Corporation as a coating to prevent penetration of the pressurizing fluid Sovasol #6. Ely [9, 13] used a paraffin wax per federal specification VV-W-95, type 1. Other investigators used various rubber and silicone sleeves applied to the specimens. Generally, paraffin was

most satisfactory.

A thin coating of nickel was used as a barrier for biaxial test at elevated temperature. The effects on strength of this coating were evaluated and considered negligible (Jortner, [29]).

CHAPTER III

MATERIALS AND METHODS

Introduction

Tests conducted were compressive and tensile uniaxial tests and multiaxial tube tests with the main emphasis on biaxial compression fracture. Uniaxial tests were performed along the three orthotropic axes to obtain the intercepts between the failure surface and the two-dimensional principle stress space. These tests also indicated the degree of orthotropy and material stress-strain relations. These uniaxial fracture strengths are the intercepts of the axes of biaxial stress space and the strength tensor ellipsoid that are used in the evaluation of the strength polynomial coefficients.

The pressure vessel method or biaxial cylinder was used for the multiaxial testing. Biaxial tubes were designed for use with emphasis on the state of biaxial compression to obtain data in the biaxial compression quadrant. The assumption was made that a higher value of strength represents more accurately the material properties, since any decrease in strength is assumed to be due to buckling, stress concentration, or instability in the arch action. In the tube tests, the stresses were considered to be the principle stresses as defined by the thin-walled approximation.

The procedures of testing presented in this chapter deal specifically with the methods used in obtaining the data presented in the figures and tables in the chapter on results. However, procedures

and devices used in preliminary investigations for the development of the test apparatus and methodology will be mentioned in the results chapter, as deemed pertinent to the test technique development. All components of the test apparatus were fabricated from salvaged material. This prevented the desired accurate description of many components like pressure regulators, seals and gaskets, and the stainless steel cylinder. However, an attempt has been made to accurately describe these components even though their origin is unknown.

Material Tested

Material available for this investigation was AGOT type EGCR nuclear-grade graphite. It has a purity of 99.9% carbon with a maximum grain size of 1/32" and a density of 1.72 g/cc. It was developed specifically for experimental high-temperature gas-cooled reactors. The billet dimensions as extruded are 4 3/8" x 4 3/8" x 51". Like most extruded graphites, AGOT is considered to have a preferred crystal orientation with respect to the extruded axis. Its mechanical properties are transversely isotropic; that is, the properties along the extruded axis (the parallel direction) are different than those lying in a plane perpendicular to the extruded axis (the transverse direction).

Machining of Graphite Test Specimens

The machinability of graphite is complicated by high tool-wear characteristics. Also, since graphite has a relatively low modulus of elasticity, its deflection from tool pressure is fairly large, making accuracy of cuts difficult. However, visually inspected surface finishes of 125 micro inch rms or better were obtained. According to the carbon and graphite handbook, surface finishes of 63 to 250 micro inches can be obtained at cutting depths of 0.0005"to 0.005" at cutting speeds of 1000 ft./min. The best tolerances for the outside diameter in a turning operation are 0.0004" (The Industrial Graphite Handbook [44].)

The biaxial tubes and the uniaxial tensile specimens both had reduced gauge sections with large radii. Gauge sections on all specimens were left as machined. The transition between the gauge section and the ends were made by the use of a tool fabricated with a $2\frac{1}{2}$" radius. This prevented any ridge or undercut at the transition between the gauge section and the radius. Since no appreciable local yielding occurs with graphite, even a small geometric imperfection could cause premature failure.

Separate parent blocks were used for the uniaxial tension and compression specimens. Specimens oriented with their axes parallel to the longitudinal axis, the parent billets, were of sufficient length to allow two specimens to be made from one turning. Machining of the uniaxial specimens sawed from the parent billet was done between a four-jaw chuck and a live center. Uniaxial compression specimens were right circular cylinders without reduced gauge sections. Uniaxial

tensile test specimens had a tapered gauge section. They were machined to the outside diameter and then the radius tool was used to reduce the gauge section to the desired diameter and then moved laterally to obtain the correct gauge section length. This provided the necessary smooth transition from the gauge section without stress risers.

Fabrication of the test cylinders from the extruded 4 3/8" x 4 3/8" x 51" billets was accomplished with a lathe by using basically standard machine shop practices. A 12" length of the extruded sections was the basis for the large cylinders, and 2" x 2" blocks were used for the small cylinders. They were both machined in a similar manner. The blocks were centered in a four-jaw chuck then turned to the correct outside diameter. A drill followed by a boring bar was used to cut the ID to the proper dimension. The taper for the gauge section was made by feeding a tool with a $2\frac{1}{2}$" radius to the proper outside diameter for the gauge section. With this setting, the tool was moved longitudinally with respect to the specimen for the gauge section length. The cylinders were then pared off to the correct length and the sharp corners on the inside were broken to facilitate easier installation of the O-ring. This method for obtaining the "neck down" of the cylinder tends to avoid a ridge or undercut at the point of transition between the gauge section and the radius. For brittle materials, even a small imperfection at this point of high stress concentration may initiate failure.

There were two primary multiaxial tube geometries were used in these tests (Figure (3-1)). The small cylinder geometry was similar to that used by previous investigators with a D/T (Diameter/ Wall Thickness) ratio of 13 and a L/D (Length/Diameter) of 4. The large

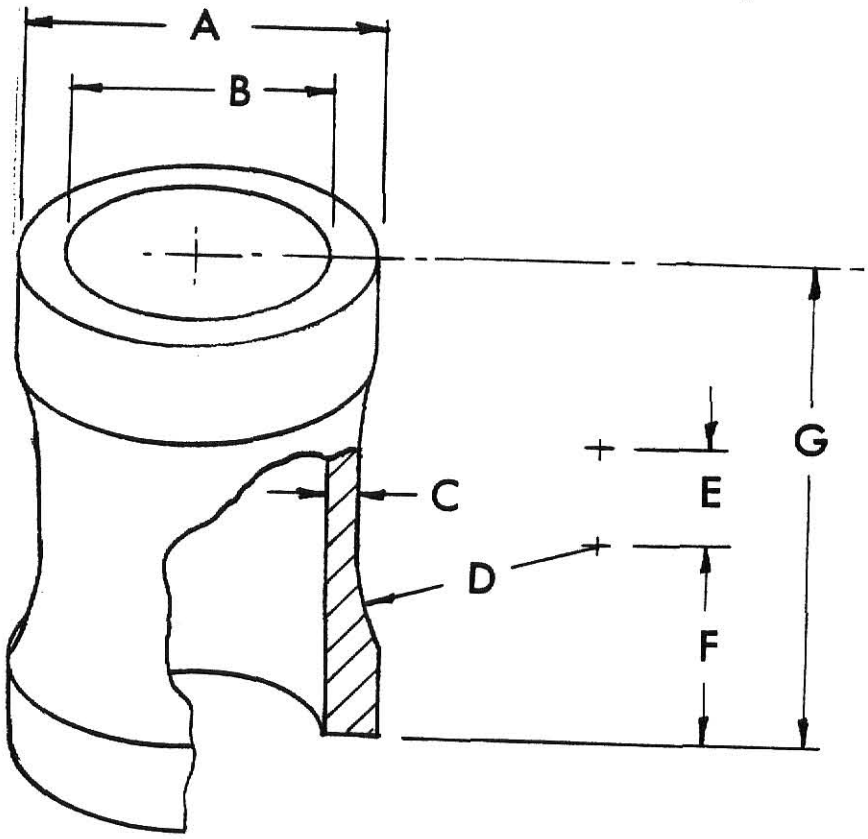

	A	B	C	D	E	F	G
Large Cylinder	3.75	2.75	0.25	2.50	1.00	2.00	5.00
Small Cylinder	2.00	1.50	0.125	2.50	1.00	1.25	3.50

Figure 3-1: Biaxial Test Specimen Geometries (in Inches)

cylinder dimensions were chosen to obtain more accurate data under cc load with a D/T ratio of 12 and a L/D of 1.6. Considerations in choosing specimen dimensions were the ratio between radial stress and hoop stress as affected by the D/T ratio. The length adversely affects buckling load yet increased length is needed to minimize extraneous stresses created by the end conditions. The transition from the gauge section was designed to minimize stress concentration yet assure that fracture takes place in the gauge section.

Most of the cylinders were measured at two perpendicular points at the center of the gauge sections for both OD and ID. To obtain better accuracy in determining wall thickness, a direct measurement device was used. This was accomplished by using a dial type micrometer with a resolution of 0.0005". This micrometer with a spherical extension was used in conjunction with a $\frac{1}{2}$" ball bearing mounted on a rigid arm constructer for this purpose. The cylinder wall was placed between the ball bearing and the micrometer and tilted to obtain accurate readings. Wall thickness measurements were usually made at eight points on the cylinder at four points 90^{o}apart located at the end of each cylinder.

Design and Fabrication of Test Apparatus

The loading of the biaxial cylinders involves pressurizing various regions of the test fixture. The test fixture (Figure (3-2)) is of stainless steel and is rated at a maximum operating pressure of 5000 psi. It was originally an hydraulic component with gas and fluid separated by a piston and has an excellent inside surface finish. Various end platens were machined from 2024-T6 aluminum. The single

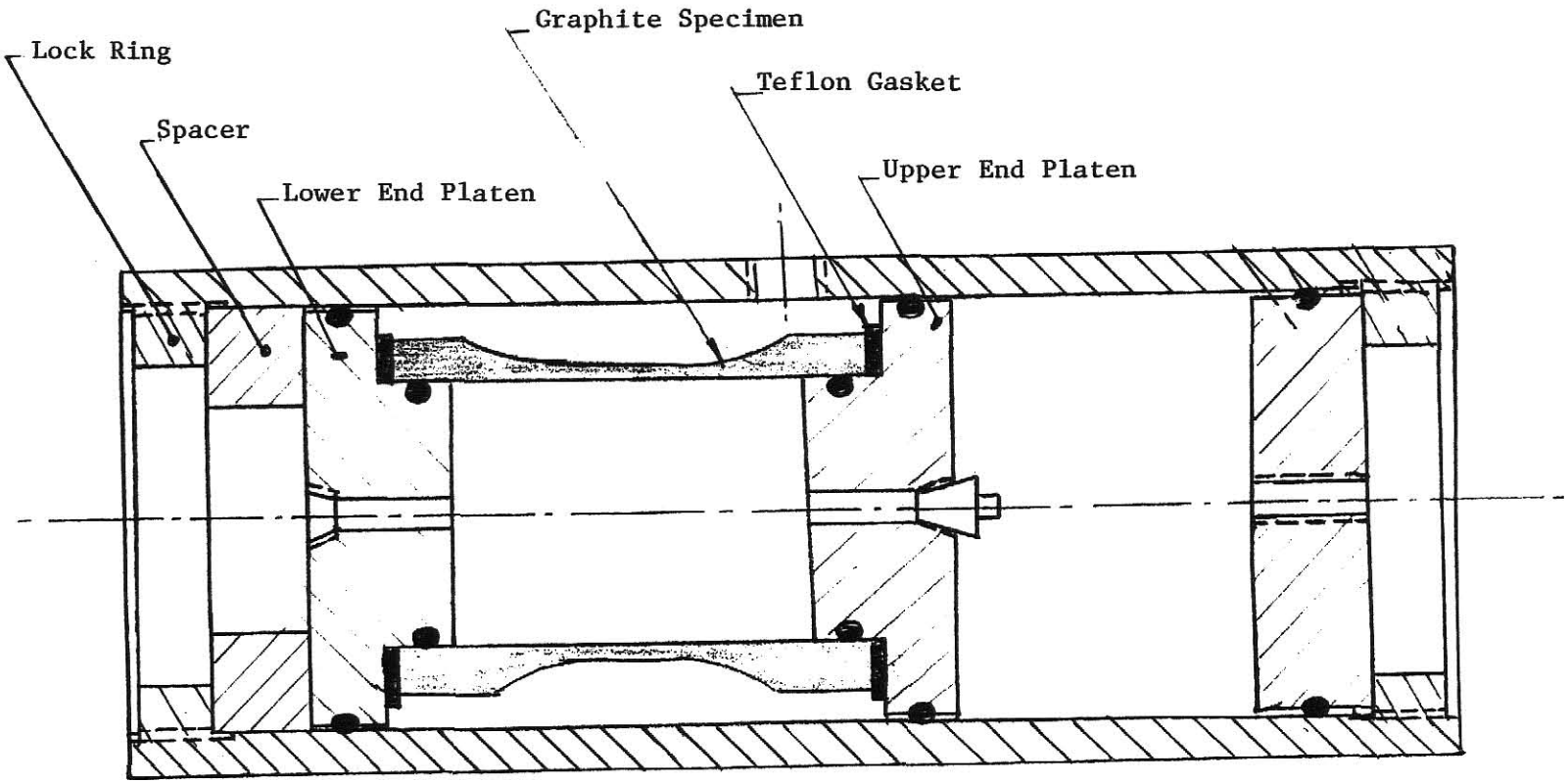

Figure 3-2: Stainless Steel Testing Cylinder with a Large Graphite Biaxial Cylinder

O-ring seal of the end platens allowed for some correction for any misalignment due to the specimen itself, the teflon gaskets, or the adhesive bond.

The schematic of the loading apparatus is shown in Figure (3-3). The basis of the system is the two Hoke pressure regulators with compressed nitrogen gas used as the pressure source. Various crossover and relief valves permitted accomodation of different loadings. Any pressures that did not exceed 400 psi were read on the 400 psi gauge; otherwise readings were taken from 3000 psi gauges. The 0-400 psi pressure gauge was calibrated by the use of an Ashcroft deadweight tester to 350 psi. This gauge in turn was compared with the other gauges to 400 psi and they were compared with each other and a third gauge believed to be correct.

Each of the two pressure-channels could be controlled separately or a single regulator could be used to provide equal pressures in each system. Radial loading, i.e., loading from the origin, along a radial line representing the load path was approximated where applicable by incrementing each pressure channel by a proportional amount. The larger pressure increment never exceeded 50 psi. The pressure regulators provided constant pressure independent of gas flow. This corresponds to constant stress in the specimen even with leakage or strain. The pressure regulators also retained their highest set pressure when source pressure rapidly dropped at failure. Since failure of the specimen was catastrophic, the system was repressurized to determine the failure pressures. The pressure regulator could be regulated easily in five psi increments. Loadings under the control of a single regulator had a pressure increase rate of 25 psi per second.

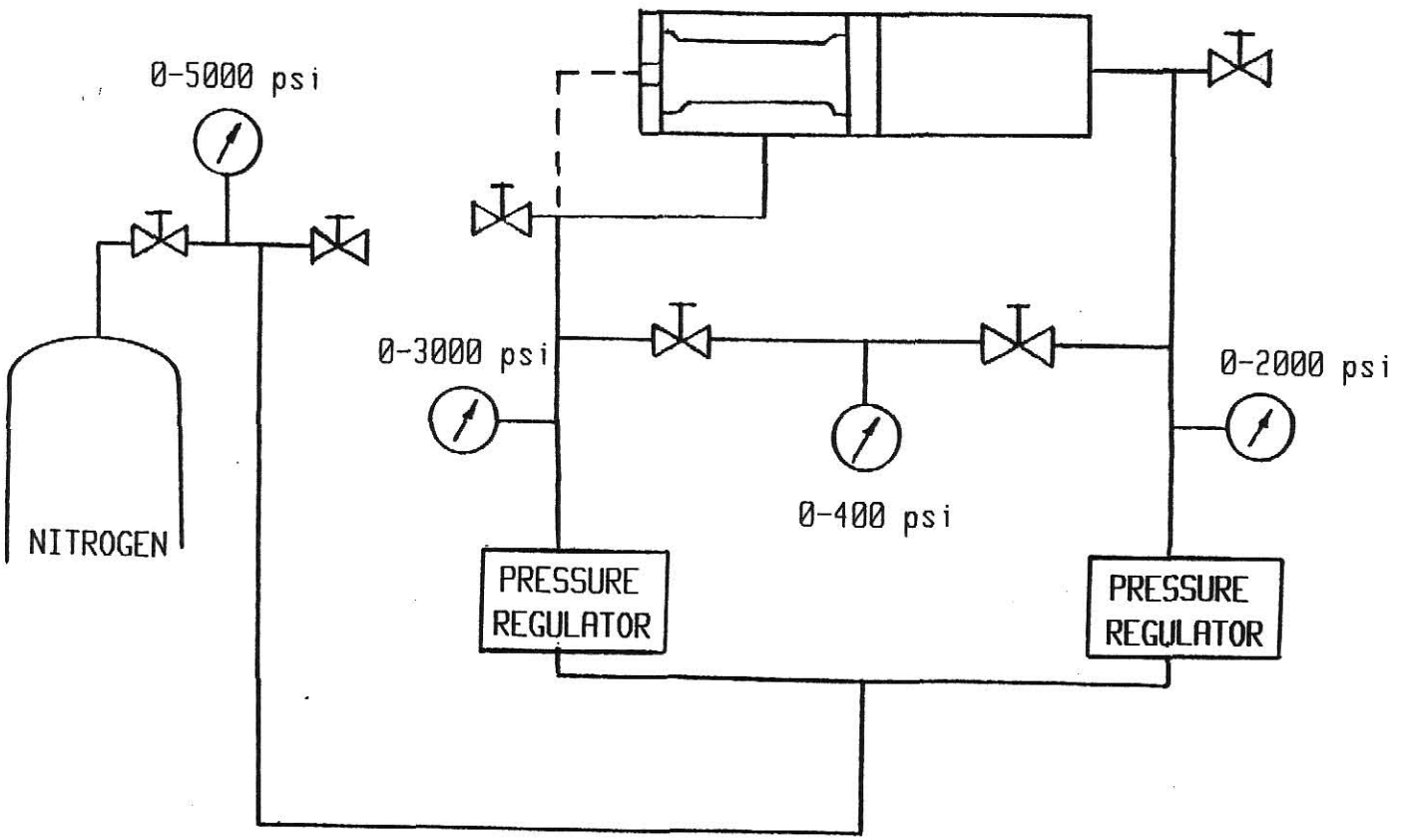

Figure 3-3: Schematic of the Pressure Application Apparatus for Biaxial Testing

Using both regulators, the step function was increased at approximately 100 psi per minute. When pressure was applied to both the inside and the outside of the cylinder, the channel with the lower pressure was required to have a continuous bleed-off to prevent any gas leakage across the wall from increasing the lower pressure. Initially, the entire system including the lines past the point of the regulator was filled with water to reduce the energy release upon fracture. Later it was expedient to use water only in the portion above the upper end platen.

For the large cylinders with axial compression, i.e., all loadings below the horizontal axis in the two-dimensional stress space, teflon gaskets were used. A steel cylinder was used inside these test specimens to prevent post fracture damage. Neoprene gaskets between the small test cylinders and their end platens were used. Both cylinders were sealed by the use of O-rings in the inside $\frac{1}{4}$" from the end. A coating of silicone vacuum grease was used to aid in sealing. Teflon gaskets (Figure (3-2)) were 0.125" thick and were rigid enough not to flow into any surface pores and cause small tensile stresses at the ends.

All cylinders under axial tension were adhesively bonded to end platens. The adhesive layer was approximately 1/8" thick and is the same as that used for uniaxial tension specimens. This end condition, of course, is different than the teflon gaskets and O-ring seals of the compression specimen.

Strain gauges were applied to the inside and outside of the gauge section of five test cylinders. Readings from these gauges were taken as a function of applied pressure or axial load. Some strain gauges

were transversely mounted. Compression readings were made using a variety of boundary conditions. These include two O-ring placements at the end of the specimen and a teflon wafer. Limited stress-strain data were recorded for other loading conditions with both axial and transverse gauges.

In the hoop compression stress state, strain gauge lead wires from the outside of the cylinder were passed through a small section of a tube filled with epoxy and the inside strain gauge lead wires passed through the atmosphere vent. A strain gauged aluminum cylinder of the same inside diameter as the small graphite cylindrical specimen was used in preliminary evaluation of sealing and loading techniques.

Sealing Procedures

Theoretically, solid carbon should have a density of 2.12 g/cc. AGOT graphite has a density of 1.72 g/cc indicating that 19% of its volume is voids. With applied pressures on the order of 1000 psi, localized tensile stresses can initiate fracture (Jortner [29]). This is referred to as the pore-pressure effect. A barrier was needed to prevent nitrogen penetration and any pore-pressure effects. The following five coatings were tried: paraffin, warwick wax, polyurethane, silicone, and beeswax.

Six of the small graphite cylinders were weighed then oven dried at 250°F. for eight hours to determine moisteure content; no appreciable water content was found. Each coating was applied to a small graphite cylinder of known weight. The coated cylinders and an uncoated cylinder were reweighed after they were pressurized in water for six hours at

1000 psi. They were then air dried and weighed to determine moisture content.

Paraffin wax was selected for the coating because of the ease of application, repair, and quick setup time as well as its barrier qualities. A thicker paraffin coating was made by multiple dippings in liquid paraffin, which prevented leakage at high pressures. Paraffin used to coat the cylinders was always removed from the ends so the graphite would rest on the teflon seals to prevent paraffin flow into the surface pores at the specimen ends. Nadai [33] believed that lead foil, unlike paper, "flowed" into pores at the ends of his ceramic hollow cylinders, under axial compression, and initiated failure. Specimens, particularly those with internal pressure, were coated on the inside with wax. Tension specimens, because of the adhesive, could not be coated prior to assembly. Coating of the inside of these specimens was accomplished by heating them to about 150^{o}F. and adding liquid paraffin wax through the pressure port.

Some specimens subjected to internal or external pressure did exhibit some leakage of the coating. This leakage, if at an acceptable level for pressures of 100 psi, always remained fairly constant until failure. This was noted but was not considered to have a significant effect on specimen strength. If preliminary bench tests revealed excessive leakage with 100 psi air, the system was disassembled, specimen recoated, and O-ring seals realigned.

Uniaxial Compression and Tension Procedures

Uniaxial compression tests were performed using cylindrical

specimens 1" in diameter. The test specimens with a length of 2" generally comply with ASTM proposed standards for compression testing of nuclear graphite. However, the specimens with a length to diameter ratio of 2.5 were used, as they might provide a larger zone of uniform uniaxial compression. Load was applied by the use of a Riehle 20,000-pound test machine. End conditions were steel platens on spherical seats. Load was applied in ten to 50 pound increments and recorded with corresponding strains. Strain readings were taken by using two Budd strain gauges with a gauge length of 0.25". These gauges, as for all graphite specimens, were bonded using Micromeasurements M-Bond 200 strain gauge adhesive. The two gauges were applied diametrically opposed at the middle of the specimen. One other gauge was applied transversely. The orientation of these gauges with respect to the material axes was recorded. Strain readings were taken using a Vishay switch and balance box equipped with a dial indicator.

Any failure of the strain gauge presumably due to failure of the bond was characterized by an abrupt drop followed by a continuous drop in the strain readings. Readings from strain gauges that failed were used to this point of discontinuity and then ignored. Fracture strength was characterized by an abrupt drop in load, typical of brittle materials. Specimen orientation, exact dimensions, and fracture strength were recorded.

Stress-strain data for the compressive as well as the tensile tests were statistically analyzed by applying a fifth order least squares polynomial. Polynomial coefficients for stress-strain curves representing multiple guages on the same specimen were averaged. The resulting polynomial represents the average of the multiple strain

gauge readings and characterized stress-strain relations of carbon and graphite. Strain gauge instrumentation and analysis for tensile tests were the same as for the compression specimen.

Tensile tests were chosen with the geometry as shown in Figure (3-4). The "dog bone-shaped" specimen taper was used to facilitate fracture in the gauge section and to reduce the effect of stress nonuniformities caused by any unevenness in adhesive bond. The tension specimen lengths as in the compression specimens were limited in the transverse direction due to the billet dimension of 4 3/8". It was desired to have a large cross-sectional area in order to more characteristically represent the material by minimizing size effects. The length was to allow a sufficient portion for the lathe.

With adhesive bonding, the end conditions are considered fixed. The taper reduced the effect of the shearing forces at the ends caused by the Poisson effect. The end caps (2024-T6 aluminum) were machined and drilled in one operation to insure alignment.

Two 5/8" National Fine studs were inserted into the end caps and attached to a clevice permitting the use of a cable to apply the load. The load was applied by using a test machine utilizing a 1/8" diameter stranded stainless steel aircraft cable which was just large enough to transmit the applied load. This procedure greatly reduced any bending moments transmitted from the loading source to the specimen.

The end caps were bonded to the tensile specimen with Sikadur Hi-Mod Gel, Sikastrix 390 which has a stated tensile strength of 3,000 psi (as used by Swartz [39]). The adhesive was applied to the specimen and end caps and fixed between the centers of the lathe. Rotation of the chuck at 100 rpm caused the generation of different rotational

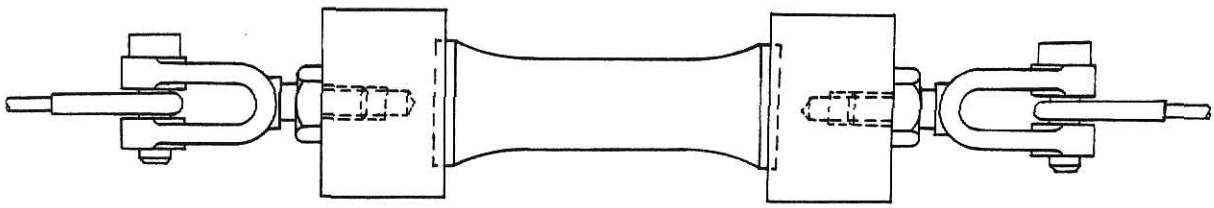

Figure 3-4: Uniaxial Tensile Test Specimen and End Caps with Cable Attachment

velocities across each of the adhesive bonds. This allowed any voids in the adhesive to dissipate and permitted self alignment with respect to the end caps. Techniques used in making tensile tests helped assure uniform loading and reduced moment loadings due to misalignments in load application. All procedures of this test unless otherwise noted conformed to the ASTM C56565T standards for tensile testing.

Biaxial Fracture Test Procedure

Biaxial stress space is represented in a plane with the axis corresponding to principle stresses in the hoop and axial direction. A radial stress across the cylinder wall would be represented by a third axis in three-dimensional stress space. The four quadrants in the biaxial stress space are t-t, t-c, c-c, and c-t. The first of these letters designates either compression or a tension stress state in the transverse or hoop direction. The second specifies the axial or longitudal stress state. The apparatus primarily designed for the c-c stress state can be used for all loadings. This involves the application of nitrogen gas in various portions of a test apparatus (Figures (3-2) and (3-3)). Pressure above the upper end platen provides an axial compression force on the test specimen. Pressure differences across the specimen wall provide positive and negative hoop stresses as well as an axial tension load. Application of pressure to the upper portion and outside portion of the test cylinder is accomplished through ports at the top and side of the test apparatus. Pressure is applied to the inside of the test cylinder through the bottom port (used as a vent to the atmosphere during c-c tests) or through a port

on the top of the upper end platen which is accomplished by sealing the hole on the bottom platen.

As pointed out earlier, boundary conditions play an important role in stress distribution. Four sets of teflon seals were rotated for each test as not enough seals were available to permit a new set for each cylinder. However, measured permanent compression of the teflon gaskets after being used several times decreased less than 10% in thickness. These seals were carefully inspected after each test for nonuniformities. A thorough cleaning of the entire apparatus was necessary after each fracture to insure that no graphite particles interfered with the O-ring seals or increased friction.

In the tension-compression quadrant and the lower portion of the tension-tension quadrant the hoop tensile stress was created by pressurizing the inside of the test specimen. The ratio of the internal pressure to the average hoop stress for the large and small cylinder was 6 and 6.5 respectively. Regions in the upper c-c and c-t stress quadrant required various applications of external and internal pressure. The applied pressure on the specimen creates a compressive stress in the radial direction at that surface. This means, for example, that in the c-c quadrant of the biaxial stress space for the large cylinder the maximum radial stress at the surface is 1/6 of the hoop stress.The distribution of the radial stress in the specimen wall from its known values on the surface of the specimen that are numerically equal to the applied pressures is unknown.

For the purpose of compatibility with other investigators, hoop stresses were based on uniform stress distribution or the thin-walled approximation. For the large cylinders with external pressure, this

value was 14% lower than the peak stress and 1% lower for large cylinders under internal pressure, as calculated by Lame's equation for thick-walled cylinders. The equation used to calculate these hoop (transverse direction) stresses and axial (parallel direction) stresses are:

$$\sigma_A = \frac{(P_o d_o^2 - P_i d_i^2) - (P_o - P_t)d^2}{(d_o^2 - d_i^2)} \qquad (3\text{-}1)$$

$$\sigma_H = \frac{(P_i - P_o)(d_o + d_i)}{2(d_o - d_i)} \qquad (3\text{-}2)$$

where:

σ_H = hoop or transverse direction stresses.

σ_A = axial or parallel direction stresses.

$d = 4.3778$ = inside diameter of the stainless steel testing apparatus.

d_o = outside diameter of the gauge section of the graphite test cylinder.

d_i = inside diameter of graphite test cylinder.

P_t = pressure above the end piston.

P_o = pressure outside the graphite test cylinder.

P_i = pressure inside graphite test cylinder.

In biaxial stress space the strength tensor (2-1) becomes:

$$F_1\sigma_1 + F_3\sigma_3 + F_{11}\sigma_1^2 + F_{33}\sigma_3^2 + 2F_{13}(\sigma_1\sigma_3) = 1 \qquad (3\text{-}3)$$

four of these constants (F_1, F_3, F_{11}, F_{33}) are evaluated by using

uniaxial tests. The measures of the uniaxial tensile strengths in the directions of the $x_1 = x_2$ (transverse direction) and x_3 (parallel direction) axes are X_t and Z_t. Uniaxial compression strengths in these directions are X_c and Z_c. Equation (3-3) gives:

$$F_1 = \frac{1}{X_t} - \frac{1}{X_c}$$

$$F_3 = \frac{1}{Z_t} - \frac{1}{Z_c} \qquad (3\text{-}4)$$

$$F_{11} = \frac{1}{X_t X_c}$$

$$F_{33} = \frac{1}{Z_t Z_c}$$

The evaluation of F_{13} can be accomplished by the use of off axis sheer strengths (Huang and Kirmser [23]) or by the use of a biaxial test (Tang [40]). Let o_3 = axial stress, and σ_1 = hoop stress, and α is a proportional constant defined by:

$$\sigma_1 = \alpha \sigma_3$$

Let B denote the value of o_3 at failure. Then Equation (3-3) yields:

$$F_{13} = \frac{1}{2\alpha B^2}\left[1 - B\,(\alpha F_1 + F_3) - B^2\,(\alpha^2 F_{11} + F_{33})\right] \qquad (3\text{-}5)$$

where the constants F_1, F_3, F_{11}, and F_{33} have been determined by Equation (3-4).

CHAPTER IV

RESULTS AND DISCUSSION

Introduction

In this chapter the results of experiments described in Chapter III are presented. In addition, results as well as details of procedures used in the preliminary stages of these investigations are included. These topics are presented primarily in the section dealing with the evaluation of the test apparatus. They pertain primarily to test techniques. This information although not germane to an understanding of the main body of the thesis should be valuable in conducting further investigations of this type. It is also believed that the discussion of these preliminary results, even though inclusive, provides valuable information.

The uniaxial compression and tension tests are discussed separately but results of these tests are included in the graph with the biaxial fracture data in two-dimensional stress space for the sake of comparison.

Evaluation of Biaxial Test Apparatus and Preliminary Tests

Results from the first seven biaxial tests are not reported as they were used to evaluate loading procedures, sealing capability of the internal O-rings, and the accuracy of determining the failure

points. Load paths for these first seven cylinders were not necessarily radial and strain rate and history varied. In addition, a gauge protector that limits pressure readings was unknowingly set at a level below fracture pressure.

The use of various stages of needle valves to provide pressure regulation proved to be successful in regulating pressure and maintaining pressure even in the presence of leaks, and for retention of the highest pressure value. After experimenting with the trial specimens, it was decided not to use water in contact with the specimens.

The system with the aluminum control specimen was pressurized in the biaxial compression mode to a bottle pressure of 2300 psi. Analysis of the stainless steel test cylinder indicated that tests could be conducted with pressures of 3000 psi which was presumed the upper limit of the pressure regulators.

Results with different cylinder orientations with respect to the end platens did not show any change in relative strain readings from different points on the cylinder. These results, while not conclusive, indicate that alignment problems were not a factor. The use of a piston with four O-ring seals unlike the end with a single O-ring seal did not allow for any rotation of the end platen. The additional sealing capacity of a piston placed against the upper end platen was not needed.

The use of the inside O-ring seal for the biaxial compression specimens proved successful even at high pressures. This method has an advantage over other methods in that sealing is not dependent upon axial load. Using a mechanical press and a 100 psi of air, the end platen could be positioned so that no axial load was exerted on the

graphite cylinder. In this configuration no axial load was exerted on the graphite cylinder. In this configuration no leakage was detected. However, under high external pressure in the c-c quadrant, leakage prohibited loading on the horizontal axis without the use of bonded end caps. Strain gauge readings did not show any change caused by the use of these seals.

The method used for obtaining stress-strain readings from general loadings of the biaxial cylinder yielded information about the test method and behavior of graphite. This procedure also provided a good method for the determination of strains on the inside and outside surfaces in a loaded cylinder. Information on buckling of the cylinders was gained by this method as abrupt changes in load distribution implied buckling. The stress-strain curve generated by this procedure provided data for characterization of graphite behavior. The repeatability of the strain readings for strain rates up to 150 psi per second indicated that stress-strain relations were insensitive to strain rate; however, this does not imply the same effect for high stresses or for fracture strength. The repeatability of the stess-strain curve within the resolution of the line on the x-y plotter also indicates that systematic errors like friction were not significant. The various strain rates and the consistency at which the recorded strain would return to the origin also implies little effect of friction from the O-ring seals. These results were also consistent with three gauge readings obtained with the aluminum control cylinder loaded with 2,000 pounds of pressure. A schematic representation of these stress-strain curves for two strain gauges on the outside, and one gauge on the inside surface of a large graphite cylinder under axial compression

stress, is presented in Figure (4-1).

The effect of four different end conditions consisting of an O-ring on either the inside or outside edge of the test cylinder and the use of a teflon gasket of uniform or nonuniform thickness on strain was attempted. Recordings of axial strains for these various end conditions did not yield a conclusive correlation between applied loads on the inside or outside edge of the cylinder and strain distribution in the wall. For different cylinders with different end conditions it seems probable that variation in material properties from location to location within the cylinder as well as strain gauge variation complicated determining the effect of end conditions on strain distribution.

The output of the strain-gauge balance box did not offer sufficient linearity to allow it to be used with the x-y plotter for strain readings to failure. However, the use of another DC amplifier could have provided the necessary range to allow the recording of biaxial stress-strain relations.

If more strain gauges had been available at strategic locations throughout the cylinder, it may have been possible to more accurately characterize strain distribution. However, even with such a system the strain distribution is expected to be a function of the magnitude of the applied load as well as type of load application. Such an evaluation involving the strain response might have yielded not only multiaxial stress-strain responses but would also have contributed to the formulation of constitutive relations, and to the design of the test procedure, specifically cylinder geometry and load conditions.

The buckling load of the thin cylindrical shell in the hoop and

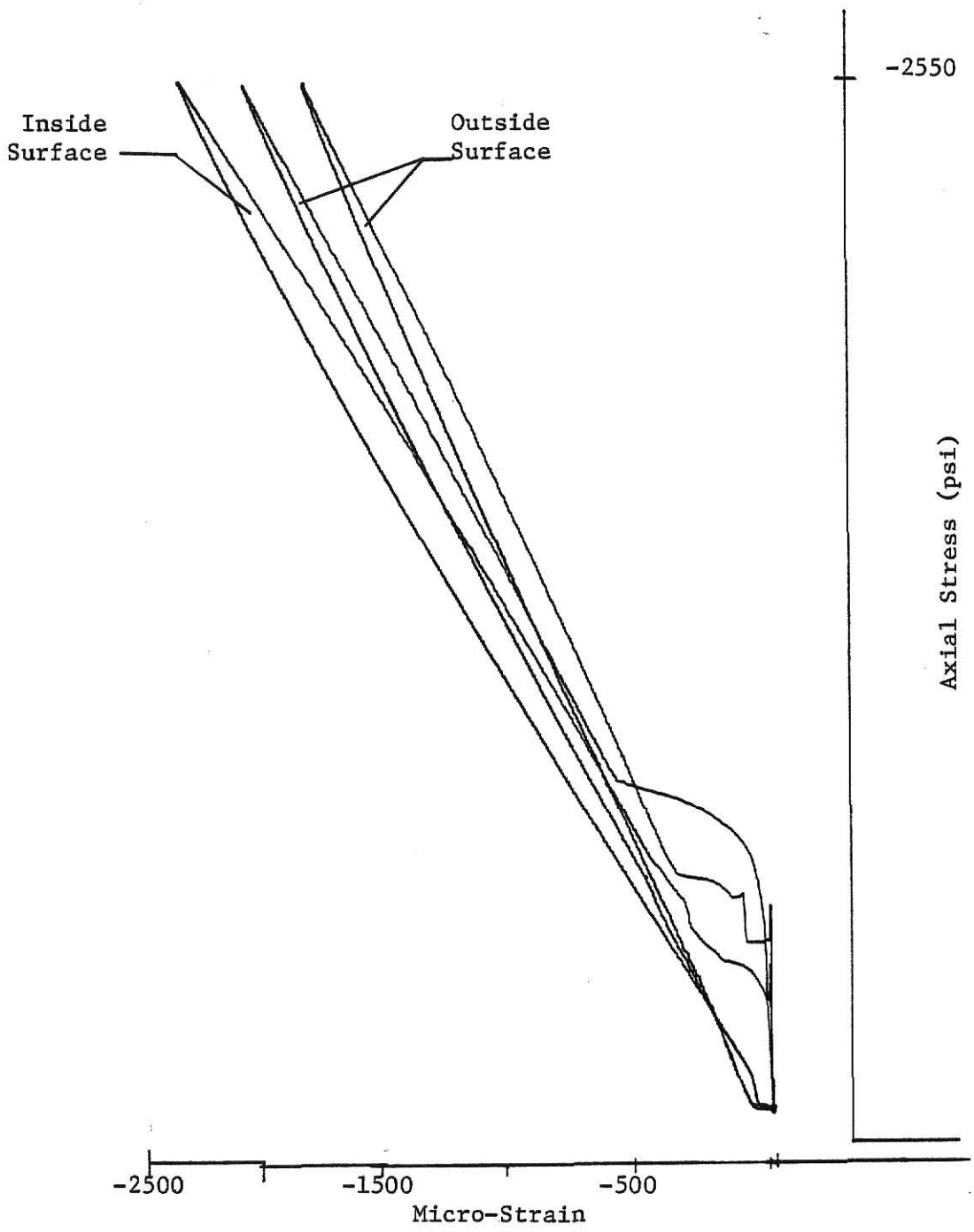

Figure 4-1: 3 Strain Gauge Readings for a Large Graphite Cylinder Under Axial Compression

axial directions was given by Timoshenko [42] where the value of E was taken in the plastic region. This value, at high loads, yields the most conservative buckling loads. Another approach to buckling was taken by using design criteria presented in the Shell Analysis Manual. As presented in this reference and Jortner [29], there are large deviations in the buckling analysis with even the small geometric deviation from the perfect cylinder. Some experimental variations in thin metal cylinders with identical geometry are as high as 500%. Analysis of thick-walled cylinder buckling is also complicated and analysis is largely based on emperical observation. Because of Jortner's necessary simplification in his buckling analysis, he considered his results to be of qualitative use. Considering Jortner's results, it is not deemed necessary to do an elaborate analysis on the cylinders with the taper and complicated end conditions as difficulty of this analysis was considered to be prohibitive. However, using linear assumptions and the conservative approximation of assuming uniform wall thickness of the gauge section, a buckling analysis on test cylinders was performed using the Shell Analysis Manual.

Results of this analysis, although of uncertain accuracy, do indicate that critical buckling loads for the large test cylinders are 1/3 to 4 times larger than those biaxial graphite cylinders used by other investigators.

The evaluation of these preliminary tests demonstrates the biaxial loading apparatus and method to be workable, accurate, and capable of applying necessary loads.

Sealing Tests

The data reported from the sealing studies (Table [1]) were for the small graphite specimens. No change in the mass of these specimens indicated that water was not initially present. Macroscopic inspection of all specimens after coating revealed no defects in the paraffin seal. Penetration of the coated specimens by water, which was initially planned to be used as the medium in contact with the specimens, was evaluated. The change in mass detected after exposure to high water pressure was used to gauge the effectiveness of the coatings. These results are recorded on Table (1). Besides its barrier qualities, paraffin had the advantage of being easy to apply, repair, cure in a relatively short time, and strip from the specimen ends. Under hoop pressures above 1000 psi the thin wax coating was found to crack and allow leakage. This was resolved by the use of a thicker was coating applied by multiple dippings.

After preliminary tests, it was concluded that nitrogen gas was more desirable than water as the medim to be used in contact with the specimen. If leakage of the wax coating occurred it was believed that nitrogen would have less of an effect on graphite. The release of nitrogen that had been absorbed by the water could create difficulty in pressure regulation, particularly for cyclic loadings. The energy released upon fracture of the specimen by the expanding nitrogen was directed safely through the atmospheric vent.

Pressure differences across the wall of uncoated specimens cannot be grater than about 50 psi without excessive gas flow through the cylinder wall. Uncoated and coated internally pressurized cylinders

Specimen Coating	Mass of Specimen With Coating (grams)	Mass of Specimen After Exposure to Pressurized Water
Paraffin	94.7	98.4
Warwick	92.5	96.5
Air Drying Polyurethane	92.3	94.5
Silicone	93.0	94.7
Beeswax	93.0	96.1
No Coating	86.7	97.8

TABLE 1: Evaluation of Sealing Quality of Barriers for Biaxial Tests

were submerged under water to observe gas infiltration to evaluate the thoroughness of the coating techniques. Differences in gas flow were observed from specimen to specimen and from different regions on the same specimen. Porosity correlations with strain and fracture results might yield a non-destructive parameter like sonic modulus used in other investigations that could be used to determine material strength properties.

Uniaxial Compression and Tension Tests

Exact dimensions, orientation, and fracture stresses of the uniaxial compression and tension tests are presented in Table (2). All compresion specimens were right circular cylinders and all tension specimens were of the geometry specified in materials and methods. The orientation of each specimen as to which of the three principle axis are parallel to the specimen axis is also presented. The orientation of each strain-gauge attached to the specimen is reported where applicable. The ultimate load carried by each specimen using the minimum cross-sectional area to calculate fracture strains appears in the table. Characteristics of post fracture behavior are briefly described in the last column of Table (2). Some compression specimens after fracture are displayed in Figure (4-2).

Axial stress-strain relations for compression specimens 1, 2, and 6 in the transverse direction and 10, 11, and 12 in the parallel direction, in which all strain gauges recorded consistently until failure are presented in Figure (4-3). These data points correspond to

Specimen Number	Parent Billet Axis Parallel to Specimen Longitudinal Axis *	Gauge Section Diameter (Index)	Specimen Length (inches)	Fracture Strength (p. 31)	Fracture Type **
		COMPRESSION			
1	x	0.997	2.5	5636	2
2	x	1.002	2.5	6151	4
3	x	1.001	2.0	5643	3
4	x	1.000	2.0	5989	2
5	y	1.002	2.0	6569	2
6	y	1.00	2.5	5539	4
7	y	0.999	2.5	6137	5
8	z	0.999	2.5	6328	6
9	z	0.947	2.0	5889	1
10	z	0.946	2.5	5395	4
11	z	0.946	2.5	5976	2
12	z	1.002	2.5	5517	4
		TENSION			
1	z	0.7535	2.75	2341	9
2	z	0.7515	2.75	1759	7
3	y	0.7509	2.75	1040	8
4	y	0.7520	2.75	1403	8
5	x	0.7505	2.75	769	9
6	x	0.7520	2.75	727	8
7		0.874	2.75	---	9

* z axis corresponds to longitudinal billet axis.

** 1. Longitudinal Crack.
2. Multiple cracks, longitudinal and angular.
3. Fracture at edge of specimen end.
4. Single crack at angle originating at edge of specimen end.
5. Single crack not orginating at edge of specimen end.
6. No visible fracture.
7. Fracture at adhesive bond.
8. Perpendicular to longitudinal axis at transition between radius and gauge section.
9. Failure of Fixture

TABLE 2: Uniaxial Compression and Tension Tests

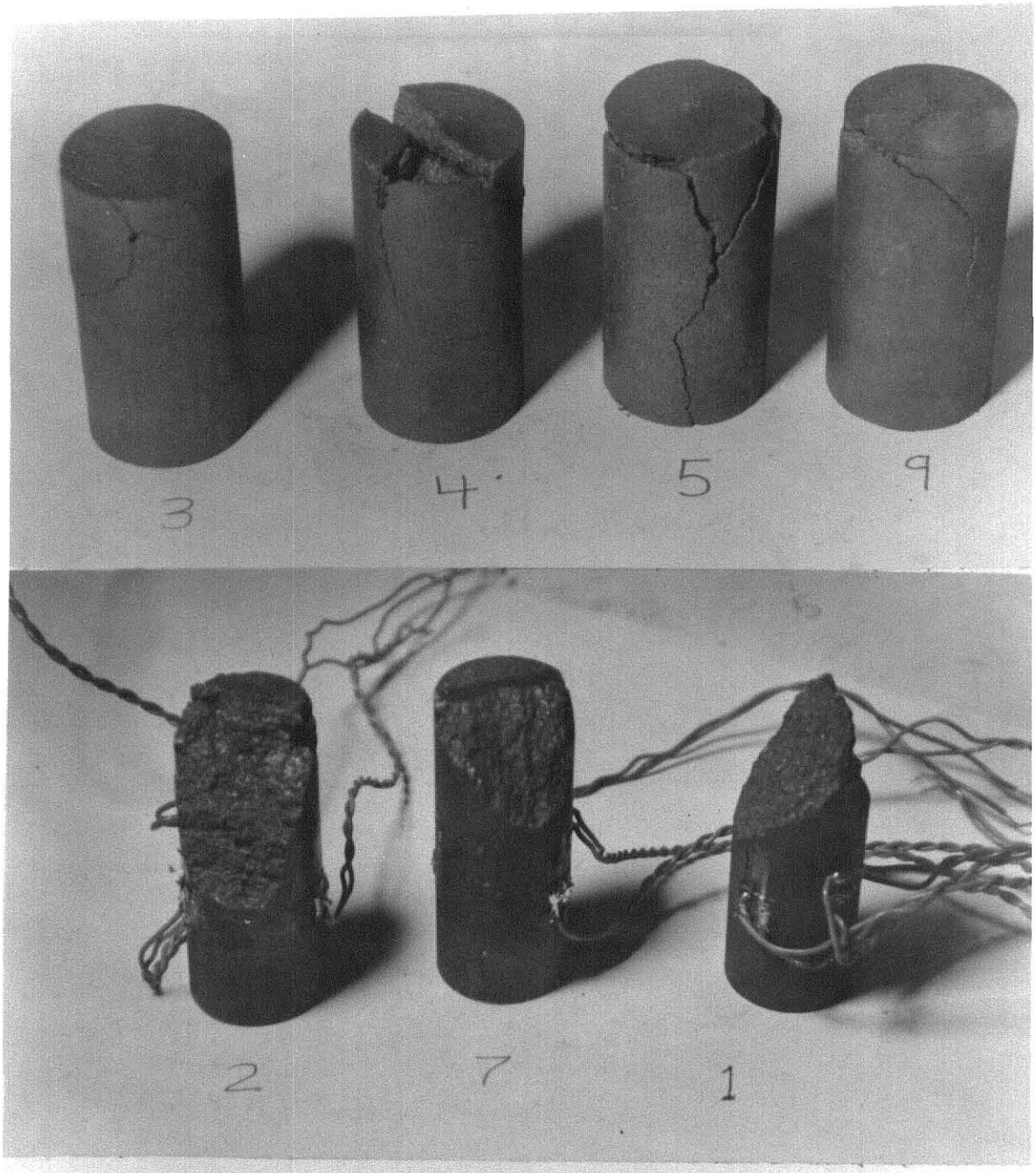

Figure 4-2 Some uniaxial compression specimens after failure (with indicated specimen numbers).

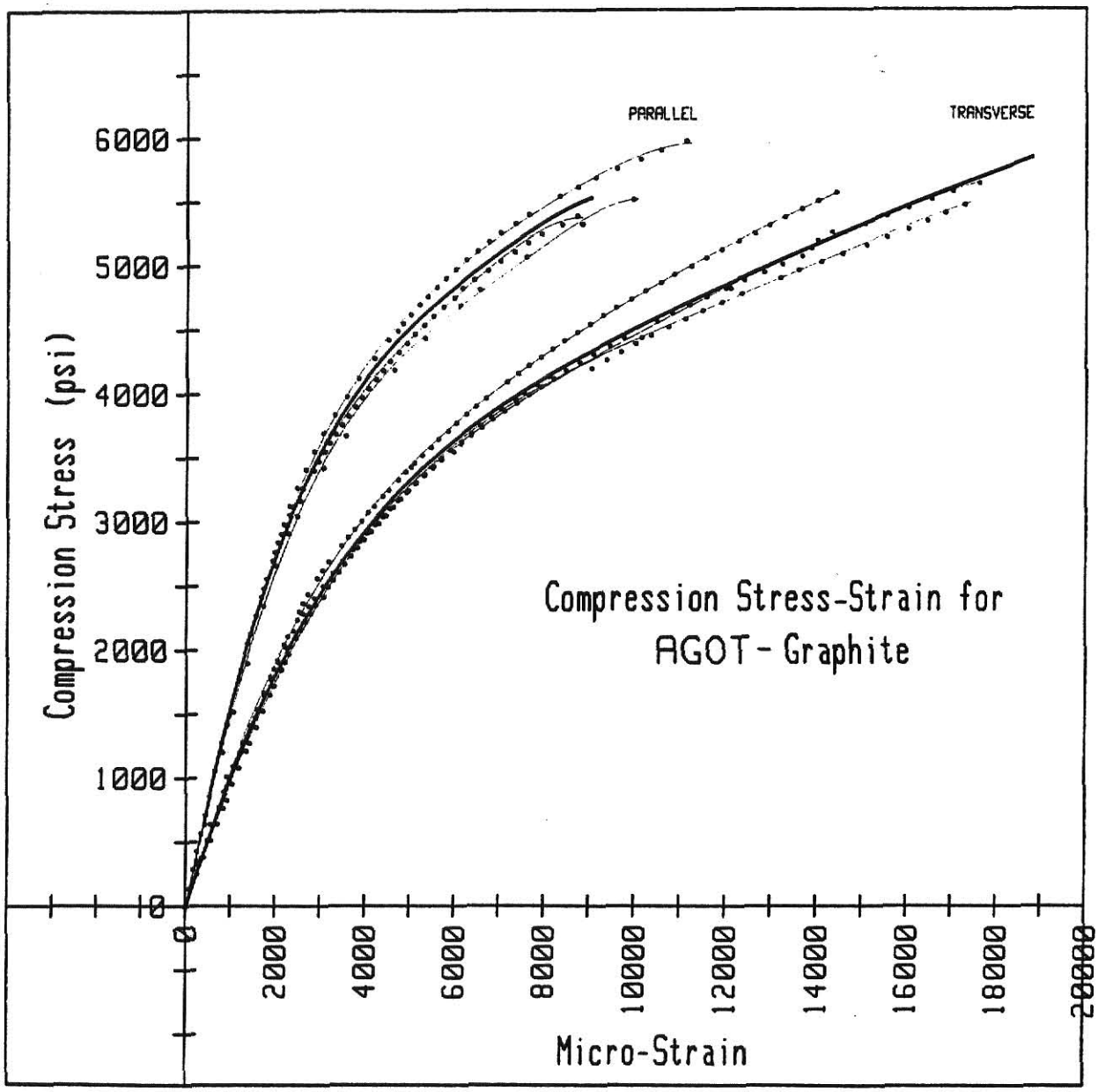

Figure 4-3: Uniaxial Compression Stress-Strain for the Parallel and Transverse Directions of Grade-AGOT Graphite

the strain gauge readings for an individual gauge. A fifth order polynomial that represents each set of strain gauge readings from one of the two axial gauges for each specimen is also presented. The heavy lines are the average of the polynomials that represent the two axial gauges and do not represent actual data points. These curves are considered to be representative of the stress-strain behavior of that particular specimen. Stress-strain relations representing the transverse and parallel directions are the upper and lower curves respectively. Strain readings on opposite sides of the uniaxial compression specimens varied by a maximum of 5% at high loads. Transverse strain gauge data were recorded to evaluate the three Poisson ratios for graphite. There was not sufficient data from the transverse strain gauges to justify reporting Poisson's ratios. However, the data from the gauges that survived indicate a linear stress-strain relation or a constant Poisson ratio.

Variation in fracture stresses of the compression specimens is within 19%. These results are consistent with those reported by Greenstreet [17] for AGOT graphite. The fracture strengths obtained are also consistent with other values reported for AGOT, considering variation in specimen strength from different billets can be this significant. In addition some of the uniaxial material testing problems such as end conditions and stress distribution are aggravated by a brittle material. There was not a sufficient number of compression tests to statistically represent the material.

Fractures originating at the ends of the compression specimens indicated the effect of high lateral friction coefficients between the specimen and the end plate. The compression specimen with a 2" length

appeared to have fractures that were more vertical in nature; therefore it is probable that this geometry yields more representative results than those from the longer specimens. Material such as teflon placed between the compression specimen and the end plate to lower the friction coefficient was reported to improve the apparent strength of the compression specimen (Peng [35]). However, a possibility of having too low a friction coefficient can also cause stress nonuniformities that cause nonrepresentative material failure.

Data for the uniaxial tension specimens are presented in Table (2). Stress-strain readings from two diametrically opposed gauges were recorded for specimen number. The results from these readings show a variation of 5%. Low fracture strength for specimens five and six were not used, as fracture of the specimen did not occur at the gauge section. It appears that specimens, particularly number one, that did not have material failures yielded conservative fracture strengths.

The fractures that did occur appeared at the transition between the gauge section and the radius. This point of discontinuity at the smallest cross-sectional area is a likely candidate for the point of maximum stress. An examination of the fractured specimens revealed no apparent surface flaws or machine errors that could have accounted for a stress concentration.

Fracture planes were generally perpendicular to the specimen axis. This type of fracture implies a tensile failure. However, this does not eliminate the possibility of failure occurring due to propagation of a crack at this point. The relatively large scatter of data from the limited number of specimens is characteristic of a brittle material in tension where a wider dispersal of data is expected than in

compression. It is not possible to statistically define the probability of failure in tension because of the limited number of specimens.

A consideration of a strength test that is to be representative of the bulk of the material is the test specimen size. A smaller gauge section has a larger surface area to volume ratio. This is a significant parameter from the aspect of the differences of material strength represented by different sample cross-sectional areas. This factor in graphite strength testing has been approached by Jortner [28], Ely [12], Greenstreet [17], and Jayatilaka [25]. Their conclusions about the significance of the gauge cross section differ. One particular mechanistic reason for failure in a strength test could be a function of cross-sectional areas. Brittle material fracture may be initiated by internal material flaws. These flaws can be crystal discontinuities or voids. This principle taken to the limit is apparent in graphite fibers that are used as the basis for graphite composite materials. The cross-sectional area of the graphite fiber is small; therefore the probability of a failure initiating flaw is reduced and strengths of 100 ksi can be exhibited by the fibers of only a single crystal strand. At the surface of some matertials the crystals are not in as strong a matrix as in the interior, and can thus initiate failure.

Biaxial Fracture Tests

Results for the biaxial test are presented in Table (3) and the corresponding fracture points are presented in biaxial stress space in Figure (4-4). Table (3) also displays exact dimensions and shape

Specimen Number *	Hoop Stress (psi)	Axial Stress (psi)	Thickness Variation (10^{-3} inch)	Outside Diameter (inch)	Fracture Type **
A	-5,410	-3,174	--		1
B	0	-5,665	--		1
C[2]	-1,665	-6,294	--		1
1[2]					
2	-6,071	-3,227	--	3.2546	1
3	-5,362	-5,691	--	3.2550	2
4	-5,741	-1,260	--	3.25544	1
5	-5,470	-5,828	--	3.2555	2
6	-3,193	-6,846	3.5,2.5,0,1	3.2550	2
7	-4,548	-7,335	-1,1,2.5,1	3.2550	1
8	-1,692	-6,569	4,0,1.5,3.5	3.2560	1
9[1]	—	—	3,3,3,3	3.2560	
10	-7,137	-1,592	2.2.2.2	3.2542	3
11[1]	—	—	--	3.2555	
12[3]	-5,480	-4,422	-2,2,3,-0.5	3.2560	2
13	-6,625	-3,886	3,3,1,1	3.2555	2
14	1472	-1332	+1	3.2555	4
15	1280	1332	--	3.2560	4
16	-4,065	-6,807	1,1,2,2 1,2.5,3,2	3.2557	1
17	+1,442	1,371	4,1,-1,2 3,1,-2,1	3.2558	4
18[1]					
19	1,388	-4,327	3,4,2,0 2,0,0,2	3.2558	1
20	-4,207	670	3.5,3.5,3.3 2,2,2,2	3.2554	1
21	-3,155	1,497	--	3.2549	6
22[4]					
23[4]					5
24	-1,442	524	3,2,0,1 3,3,0,1		6

TABLE 3: Biaxial Test Results

Specimen Number *	Hoop Stress (psi)	Axial Stress (psi)	Thickness Variation (10^{-3} inch)	Outside Diameter (inch)	Fracture Type **
25[1]					
26	1,424	-4,408	2,3,1.5,2 2,2,1,1	3.2552	4
27	-6701	-2719	1,3.5,3,0 1,3,2,-1	3.2553	2
28	-4,868	-6,300	0,0,0,1 1,0,1,1	3.255	2
30	-7,017	-1,620	1,3,3,2		1
31	-5,782	-4,916	0,2,5,3,0 -1,0,2,0		2
32[2]	-4167	-6775	-11,-9,-10,-12 -11,-11,-10,-12	3.2555	2
33	-3,072	-6499	2,2,2,2,1 2.5,2,0,2	3.2553	2
34	-5379	-11	2,0,-2,1 2,0,-2,0	3.2553	1
35	-7,288	-1620	3,4,-1,0 2,2,-1,1	3.2553	3
36	-2,855	1355	3,3,1,2 2,1,0,1	3.2553	6
37	-1,671	1,667	0,0,2,2	3.2436	5
38	0	1,753	1,1,2.5,2 -1,1,2,1.5	3.2556	6
39	0	1,823	2,3.5,2,-1 1.5,3,1,-1	3.2546	6

* 1 Specimen not tested
2 Higher than normal strain-rate due to leakage
3 Non-uniform strain-rate due to jump in regulated pressure
4 Pressure regulator problem--one pressure unknown

** 1 Excessive post-fracture damage made initial fracture type undiscernible
2 Gauge section broke into small fragments
3 Fracture at ends of gauge section
4 Full-length longitudinal cracks
5 Failure close to adhesive
6 Single circumferential crack at the transition of the gauge section

TABLE 3: Biaxial Test Results (Continued)

variations for most of the cylinders. Also presented are load stresses at failure, brief descriptions of post fracture behavior and test variations. Using the nominal OD and ID values and assuming linear stress distribution, the calculated axial or longitudal stress and hoop or transverse stress values are presented in numerical form.

Failure of all biaxial specimens occurred with no preliminary indication of pressure drop, sudden increase in leakage, or noise. Failure as in the uniaxial specimens was catastrophic. This was characterized by an abrupt drop in the applied load. In cylinders with hoop stresses, the expansion of the nitrogen gas was explosive.

Specific test specimens that were designated because of a lack of confidence in their exact values were usually the result of a malfunction in pressure application. Pressure loading increments were sometimes sudden, and if this occurred during failure, failure pressure for that particular channel could not be adequately determined.

Specimens loaded with various combinations of hoop stresses and axial tension loads were limited in number and scope, as compared with some other investigations. These points, as with the uniaxial tests, were primarily used to facilitate the application of a strength tensor theory. These cylinders, under a loading that coincides with one of the axes in principle stress space, provides an opportunity to compare uniaxial and biaxial test specimen representation of a particular fracture stress state. The specimens tested in the upper region of the c-t quadrant had failures at the adhesive. It is suspected that either specimen preparation did not allow for a good adhesive bond or this

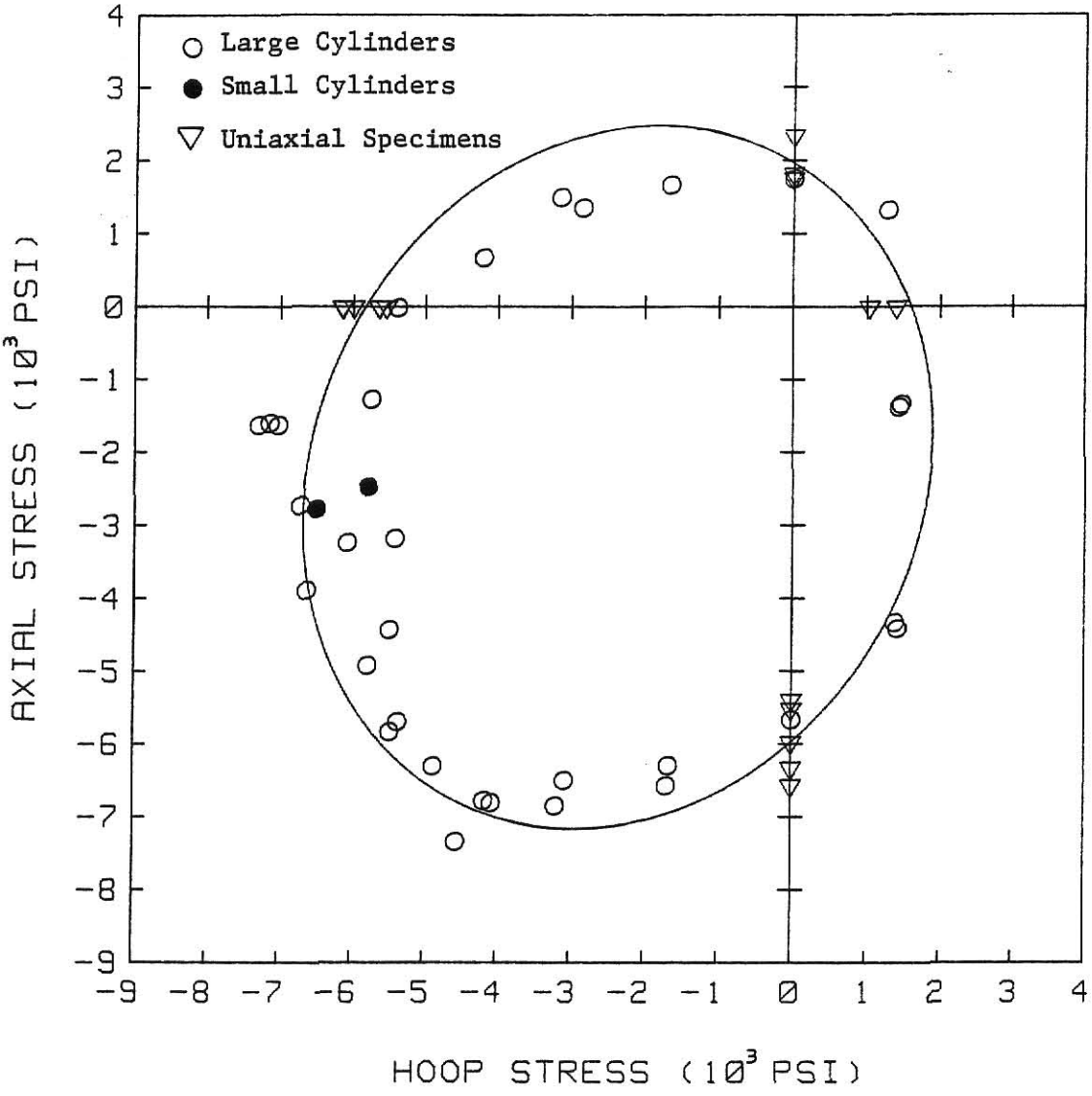

Figure 4-4: Fracture Strengths for Grade-AGOT Graphite

particular loading caused high tensile stress at the edge of the cylinder that intitiated failure. Axial tension tests conducted with the large graphite cylinders all had fractures at the transition between the gauge section and the transition radius. This failure did not occur in the uniform tensile field; therefore the fracture strengths are probably low. Many other investigators for axial tube testing in these quadrants have attempted to evolve an optimized test method and geometry. Ho's procedure is likely the best for testing graphite under biaxial tension. The large specimens used in this investigation were designed with consideration to c-c loading. The slenderness ratio of these specimens is one-fourth or less than those successfully used by others in loads involving axial tension. Testing of specimens of Ho's general type in these stress quadrants would have been of interest when compared with those presented here. The limited results presented in the upper portion of the biaxial stress space agree qualitatively with those obtained by other investigators using other graphites.

The effect of the cylinder dimension variation on strength could not be precisely determined. However, this variation is considered to be a significant factor in buckling and is a factor when considering induced bending stresses (Hassleman [19]). Other factors that affect the strain in the gauge section under most loading conditions include transverse shear caused by the Poisson effect. Circumferential moments caused by the axial load not coinciding with the gauge section also cause bending stresses. Other factors more prevalent under hoop compression caused by external pressure include bending moments or barrelling of the gauge section. All these factors are affected by the

boundary type or friction and expansion coefficients and specimen geometry. When hoop compression was desired in a particular loading condition, it was done by applying external pressure to the specimen. This affects boundary conditions by causing a longitudal load created by the action of the pressure on the radius transition portion of the specimen. The external pressure was responsible for the tensile component of the specimen load. In the most significant case of external pressure, 80% of the tensile load caused by this external pressure acts on the transition radius with the remainder on the end platen. With the presence of external pressure used in the c-t and c-c quadrants, this end effect is a significant loading parameter.

Post fracture types in the c-c quadrant varied with loading. In load paths close to the uniaxial compression axis, fractures which were in the gauge section yielded fragments that were roughly of uniform size. Loading configurations close to the hoop compression axis revealed a series of cracks upon examination. Figure (4-5) shows some biaxial tube failures.

Comparison of Results with Published Investigations

The consensus of most investigators is that premature buckling affects the acceptability of points in the c-c quadrant. While it was not possible in this investigation to obtain continuous strain readings to failure which would certainly provided some insight into buckling loads and types, the fracture data indicate buckling was not significant. Load-carrying capability of the cylinders in the compression-compression quadrant was generally as large or larger in relation

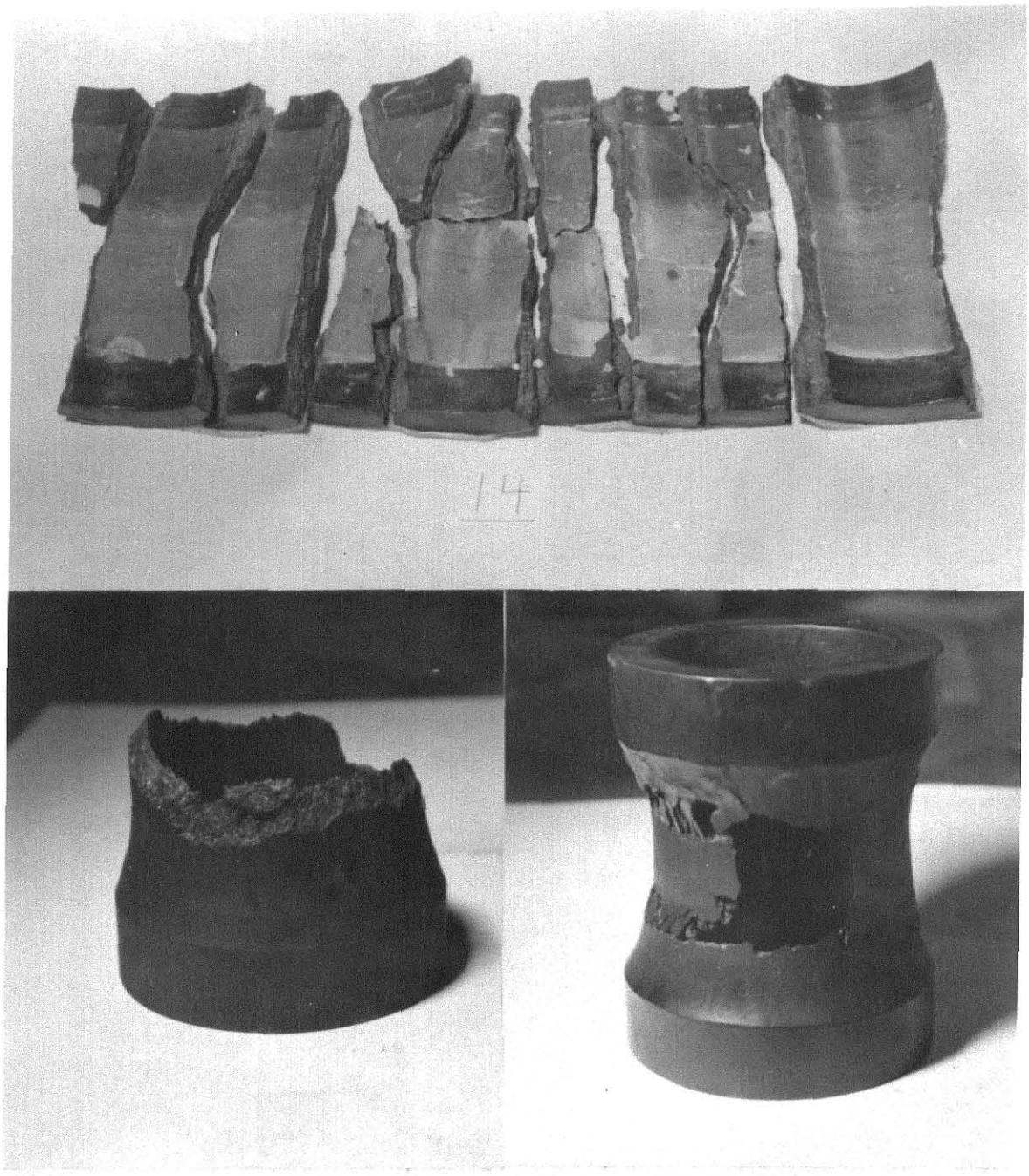

Figure 4-5 Some large biaxial cylinders after failure (with indicated specimen numbers).

to the uniaxial values as those reported by others. Most of the c-c data reported do not show multiple tests for a single load path. Comparison of present data with previously reported data does not reveal any larger variation in fracture strength. Scatter in this investigation seems small particularly when compared with variations reported in simple uniaxial tests. Increasing strength variations in the c-c quadrant as the loading approaches hoop compression are consistent with results reported by others.

Six tensor polynomials representing seven sets of data are presented by Tang [40] as being representative of the best graphite fracture data available. These strength criterial were calculated by Huang [24] and Chang [5] using experimental fracture data from eight studies [1, 13, 29, 30, 45, 46, 47, and 48]. Cursory comparisons of these data and those obtained in the present investigation can be made in Figures (4-6) and (4-4). It is evident that data in the present investigation, particularly in the compression-compression quadrant, are the most extensive. Based on the scatter and correlation with uniaxial results, the data in the c-c quadrant appear to more adequately characterize the fracture of graphite than others reported in the literature.

Figure (4-4) shows the failure criteria as calculated by using a biaxial compression test and the average values of the uniaxial results with the exception of the tensile tests for the positive hoop stress axis. The values used for calculating the failure criteria in Figures (4-7) and (4-8) are presented with the coefficients of the strength tensor polynomial in Table (4). The uniaxial strength values for Figure (4-7) are taken from Nightingale [34]. The values from Greenstreet [17]

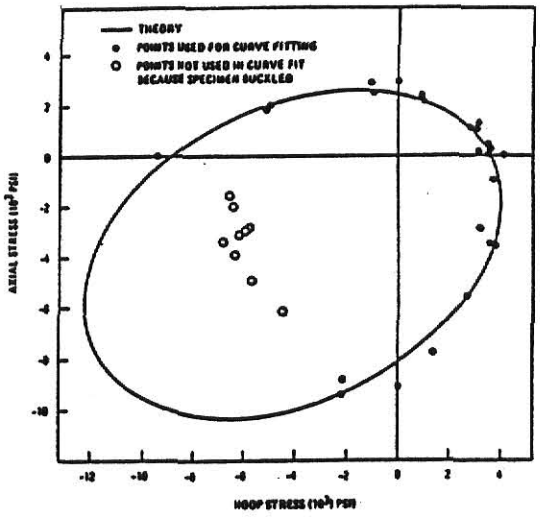

ATJ From Chang (5)

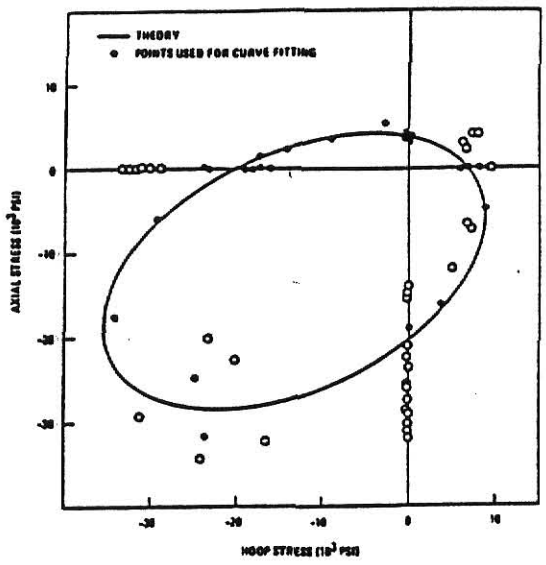

JTA From Chang (5)

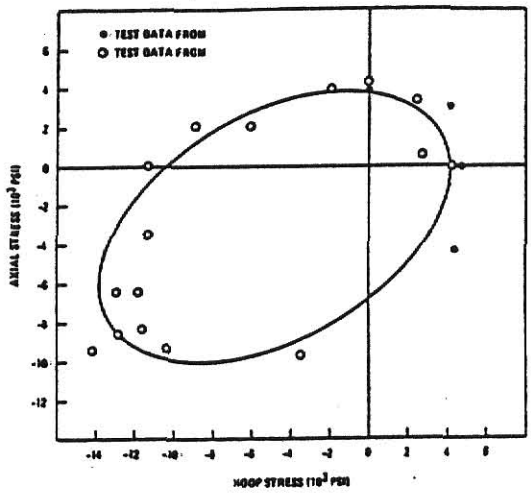

ATJ-S From Chang (5)

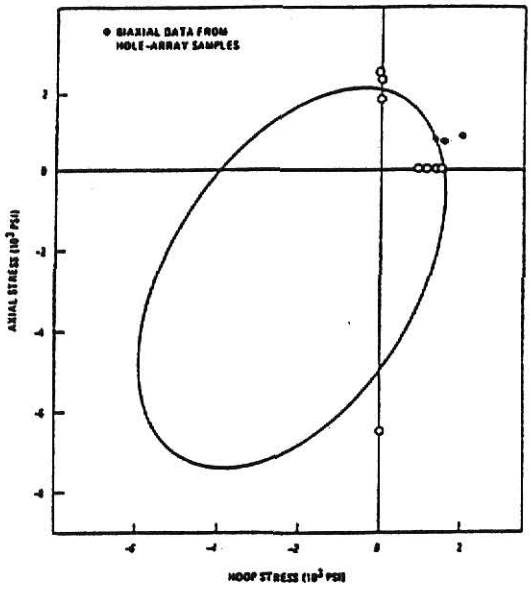

H-327 From Chang (5)

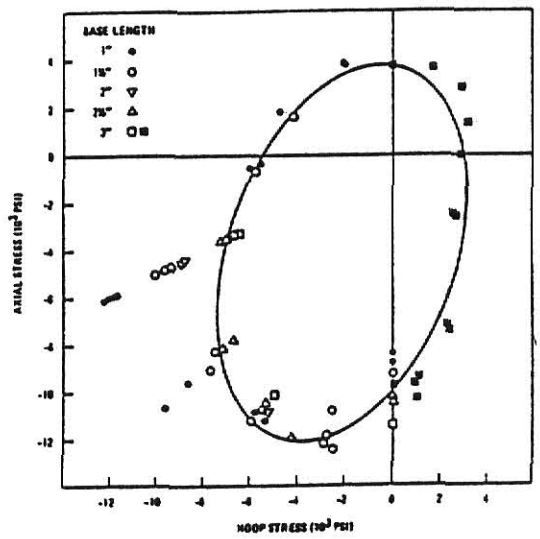

Graph-I-Tite From Huang (23)

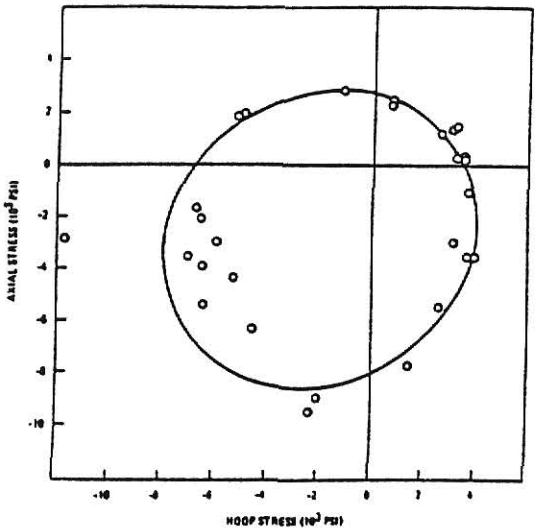

ATJ From Huang (23)

Figure 4-6: Biaxial Failure Surfaces for Various Graphites

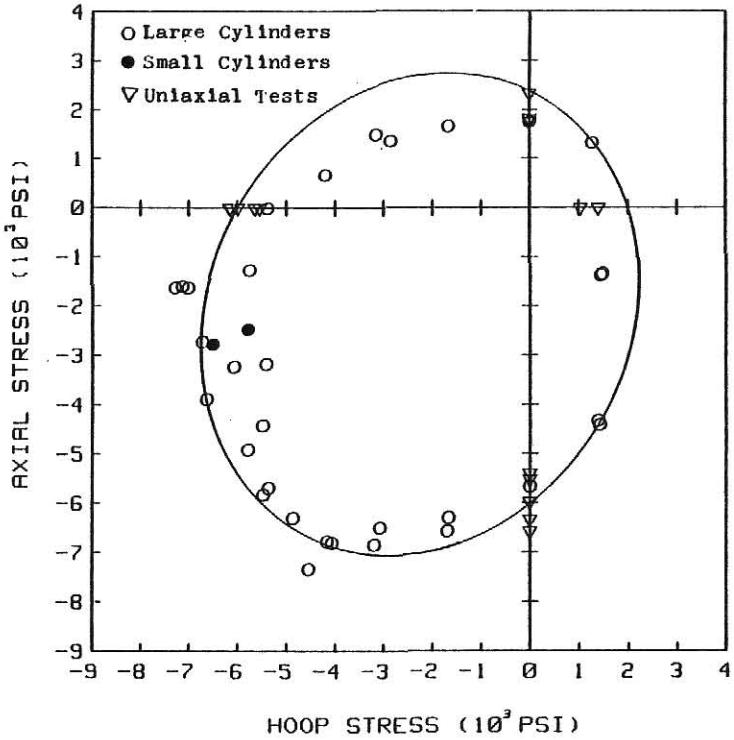

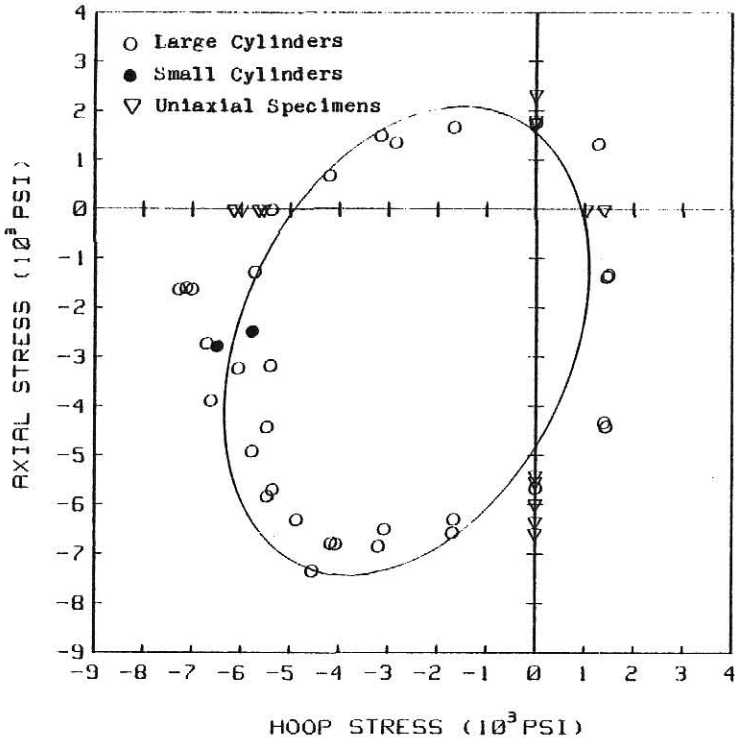

Figures 4-7 and 4-8: 2 Dimension Strength Tensors Partially Calculated from the Data of 34 and 17 , Presented with Fracture Results from Present Investigation

Figure Number	X_t (psi)	X_c (psi)	Z_c (psi)	Z_t (psi)	σ_3 (psi)	σ_3 (psi)	F_1	F_3	F_{13}	F_{33}	F_{12}
Fig. (4-4)	5,849	1,600	5,957	1,974	-6,300	-4,868	4.538×10^{-4}	3.38×10^{-4}	1.070×10^{-7}	8.504×10^{-8}	1.229×10^{-8}
Fig. (4-7)	6,000*	2,000*	6,000*	2,400*	-6,300	-4,868	8.724×10^{-4}	4.286×10^{-4}	2.180×10^{-7}	1.326×10^{-7}	-5.243×10^{-8}
Fig. (4-8)	4,930**	930**	4,800**	1,570**	-6,300	-4,868	8.724×10^{-4}	4.286×10^{-4}	2.180×10^{-7}	1.326×10^{-7}	-5.243×10^{-8}

* From [34]

** From [17]

TABLE 4: Unaxial and Biaxial Strengths with the Calculated Polynomial Coefficients for Biaxial Failure Curves

used in Figure (4-8) are averages from tests of different methods, and therefore probably represent values somewhat lower than the material strength. For both Figures (4-7) and (4-8), uniaxial values for calculating F_1, F_3, F_{11}, and F_{33} were obtained from other investigators. However, for the calculation of F_{12}, a biaxial compression test from the present investigation was used.

These investigations should help elucidate the characterization of other brittle materials which have a dearth of biaxial compression tube data. For uniaxial tests of brittle materials, variations in strength can occur even when experimental techniques and apparatus are based upon ASTM and British Standards, as they allow for different end conditions. Variations in fracture strengths in both uniaxial and multiaxial tests of the same type of graphite have been reported as well as for other brittle materials. Jayatilaka [25] concludes that careful and intelligent planning of experiments is an essential requirement, particularly for brittle materials. Addressing the variability in reported fracture strengths he states: "It is conceivable that a certain degree of unreliability in the published strength data of some brittle materials is due to the imcompetence of the personnel performing the tests. Any improvement or added sophistication in an experimental technique will not help in such circumstances, but will only lead to further wastage." In light of such statements, questions arise as to the necessity of employing elaborate test apparatus.

Many investigators emphasized the need for accurate multiaxial stress-strain readings for the formulation of graphite constitutive equations and determination of buckling of biaxial compression tubes.

The methodology to obtain continuous stress-strain readings from the inside and outside test cylinder walls was demonstrated in this investigation. If the recording equipment had been available to record data on the biaxial test cylinders, it likely would have provided insight into the much needed areas of constitutive formulations for graphite, buckling analyses, and verification of specimen stresses.

CHAPTER V

SUMMARY AND CONCLUSIONS

Summary

The fracture results for grade-AGOT graphite, both from biaxial tube and uniaxial tests obtained herein were presented in (Figure (4-4)) and discussed. The fabricated test apparatus and methodology for biaxial testing in all quadrants of biaxial stress space with emphasis on biaxial compression yielded fracture strengths that are believed to be representative of the material. The large tube geometry and methods in the c-c quadrant have a better resistance to buckling than those previously reported. In view of the extensive experimental results in the compression-compression quadrant and the consistency with uniaxial fracture strengths, these results are considered reliable as compared with others available. A biaxial strength tensor polynomial for a transversely isotropic material that is a special case of that proposed by Tsai and Wu [43], contains five components that were evaluated by the use of uniaxial strength values and a biaxial test. Except for the positive hoop stress axis, the values used in the application of the failure criteria were the averages of the uniaxial tests. Tests with graphite in this investigation were complicated by its, nonlinear, stress-strain relations, Bauschinger effect and brittle fracture of graphite.

Conclusions

Extensive biaxial fracture data, in conjunction with uniaxial results, appeared to characterize grade-AGOT graphite. These results in the c-c quadrant of the biaxial stress space, with the exception of the upper portion, do not exhibit large variations in experimental fracture values, a characteristic of buckling failure. The increase in apparent strength in loadings of predominantly hoop compression, i.e. the upper portion of the c-c quadrant, is reported in similar investigations. Fracture of these specimens at the ends of the gauge section was different than other portions of the c-c quadrant, indicating an incipient bending failure or a barreling effect. Uniaxial test results are reasonably consistent with biaxial test results. In comparison with other biaxial fracture tests, results of the present investigation are more extensive and consistent, particularly in the biaxial compression quadrant, and therefore imply a better material characterization. This is probably due to the geometry of the large cylinders that were intended to be more resistant to premature buckling failure than those investigated previously. Factors in the test methodology that can significantly influence the fracture values are all factors involved with the loading technique, particularly end conditions.

Data in other quadrants, i.e. c-t, c-c and t-c, compare favorably with other investigations which produced more extensive results in these quadrants and used optimized slender tube geometries. These results with methods similar to those proposed by Ho [20] are considered to be more reliable. With consideration given to the method

used for obtaining biaxial fracture results under axial tension, the representation of the fracture data by the tensor polynomial is good.

Uniaxial tests yielded fracture strengths required for making judgements on biaxial data and application of the failure criteria. These results also provided uniaxial stress-strain relations needed for comparison with biaxial stress-strain readings and the formulation of the constitutive relations for graphite.

Uniaxial values on the positive hoop stress axis appear to be low when compared with biaxial fracture data, particularly when these test cylinders with the tension component are considered to be a lower bound of the failure envelope. Uniaxial compression specimens with material inserted between the specimen and the end platen may have lowered latteral shearing forces at the ends caused by the Poisson effect and improved strength. Specimens with a shorter gauge length on the basis of fracture are believed to be better. Since tensile specimens have fractures at the transition radii it is believed that modification of tensile specimen geometry would perfect this test. Since the technique employed in the loading with cables and end alignment of the tensile test specimen was believed to be effective. Elimination or increase in the transition radius (traditional ASTM Standard for tensile testing because of the need for end clamping devices instead of adhesive) would have certainly created a more uniform stress field thus a better test for these uniaxial tensile specimen.

The question of the influences of buckling on biaxial compressive strength, although not as significant, still persist. However, the geometry and methods chosen in this experimental procedure have a higher resistance to buckling than others previously reported.

Continuous load deflection recording during biaxial tests with the method proven in these investigations would probably have led to more conclusive buckling information. Since analytical techniques are largely emperical and not generally adaptable to anisotropic nonlinear thick-walled cylinders, it would appear that experimental investigation of the buckling phenomena would be the most productive approach. The repeatability of strain readings from biaxial tubes demonstrate the capability of the fabricated apparatus for investigations of polyaxial material response

Bibliography

1. Babcock, S.G., S.J. Green, P.A. Hochstein, and J.A. Gum,"Dynamic Biaxial and Elevated-Temperature Properties of ATJ-Graphite," Proceedings of the Conference on Continuum Aspects of Graphite Design, Nov. 9-12, 1970, Gatlinburg, Tennessee, CONF-701105, NTIS. U.S. Department of Commerce, pp. 50-59.

2. Baker, E.H., A.P. Cappelli, L. Kovalevsky, F.L. Rish, and R.M. Verette, Shell Analysis Manual, NASA Contractor Report CR-912, National Aeronautics and Space Administration, Washington, April 1968.

3. Broutman, L.J., Krishnakumar, Mallick, S.M., P.K., "Combined Stress Failure Tests for a Glassy Plastic," Journal of Applied Polymer Science, pp.1178-1189.

4. Broutman, L.J., S.M. Krishnakumar, and P.K. Mallick, "Effects of Combined Stresses on Fracture of Alumina and Graphite," J. American Ceramic Society, 53, 1970, p. 649.

5. Chang, T.Y. and T. Weng, "A Strength Criterion for Graphite Under Combined Stresses," ASME PVP Meeting, June, 1975.

6. Cobb, H.R.W., S.J.S. Parry, and G.B. Engle, "Characterization of Production-Grade H-327 Graphite for HTER Design," Proceedings of the Conference on Continuum Aspects of Graphite Design, November 9-12, 1970, Gatlinburg, Tennessee, CONF-701105, NTIS. U.S. Department of Commerce, pp. 98-114.

7. Coffin, L.F., Jr., "The Flow and Fracture of a Brittle Material," Journal of Applied Mechanics, Trans. ASME, Vol. 72, Sept. 1950, pp. 233-248.

8. Cornet, I. and R.C. Grassi, "Study of Thories of Fracture Under Combined Stresses," J. Basic Engineering, Vol. 83, No. 1, 1961, pp. 39-44.

9. Ely, R.E., "Biaxial Fracture Stresses for Graphite, Ceramic and Filled and Reinforced Epoxy Tube Specimens," Report RR-TR-65-10, June 1965, U.S. Army Missles Command, Redstone Arsenal, Ala.

10. Ely, R.E., "Strength of Graphite Tube Specimens Under Combined Stresses," J. Am. Ceram. Soc., Vol. 48, No. 10, 1965, pp. 505-508.

11. Ely, R.E., "Strength of Magnesium Silicate and Graphite Under Biaxial Stresses," Ceramic Bulletin, Vol. 47, No. 5, 1968, pp. 489-492.

12. Ely, R.E. "Strength Results for Ceramic Materials Under Multiaxial Stresses," U.S. Army Missle Command Report RR-TR-68-1, April 1968.

13. Ely, R.E., "Strength Results for Two Brittle Materials Under Biaxial Stresses," Report RR-TR-72-11, 1972, U.S. Army Missiles Command,

Redstone Arsenal, Ala.

14. Fisher, J.C., "A Criterion for the Failure of Cast Iron," ASTM Bulletin, No. 181, April 1952, pp. 74-75.

15. Gol'denblat, I.I. and V.A. Kopnov, "Strength of Glass-Reinforced Plastics in the Complex Stress State," Mekhanika Polimerov, Vol. 1, 1965, p. 70; English Translation: Polymer Mechanics, Vol. 1, 1966, p. 54, Faraday Press.

16. Grassl, R.C. and I. Cornet, "Fracture of Gray Cast-Iron Tubes Under Biaxial Stresses," Mechanical Engineering, Vol. 70, 1948, p. 918.

17. Greenstreet, W.L., J.E. Smith, and G.T. Yahr, "Mechanical Properties of EGCR-Type AGOT Graphite," Carbon, Vol. 7, 1969, pp. 15-45.

18. Griffith, A.A., "Theory of Rupture," Proc. 1st Int. Congr. of Appl. Mech., Delft, 1924, pp. 55-63.

19. Hasselman, D.P.H., "Bending Stresses in Out-of-Round Uni-and Multiaxial Internally Pressurized Strength Specimens," Experimental Mechanics, Vol. 9, Nov. 1969, pp. 527-528.

20. Ho, F. "Specification for Biaxial Stress Test," GA Document No. 902984, April 20, 1977.

21. Hoffman, O., "The Brittle Strength of Orthotropic Materials," J. of Composite Materials, Vol. 1, No. 2, April 1967, pp. 200-205.

22. Hu, K.K., S.E. Swartz, and C.J. Huang, "A Proposed Generalized Constitutive Equation for Nonlinear Para-isotropic Materials," Research in Nonlinear Structral and Solid Mechanics, Research-in-progress Papers Presented at a Symposium Held at Washington, D.C., October 6-8, 1980, NASA Conference Publication 2147, pp. 187-196.

23. Huang, Chi-Lung, and P.G. Kirmser, "A Criterion of Strength for Orthotropic Materials," Fibre Science and Technology, Vol. 8, 1975, pp. 103-112.

24. Huang, C.L., "On Strength Function for Anisotropic Materials," Proceedings of Symmetry, Similarity, and Group-Theoretic Methods in Mechanics, The University of Calgary, Canada, 1974.

25. Jayatilaka, A., Fracture of Engineering Brittle Materials, Applied Science Publishers, Ltd., London, 1979.

26. Jones, R.M. and J.G. Crose, "SAAS-II-Finite Element Analysis of Axisymmetric Solids," Air Force Report No. SAMSO-TR-68-455, September 1968.

27. Jortner, J., "Biaxial Mechanical Properties of AXF-5Q Graphite to 4000° F," Proceedings of the Conference on Continuum Aspects of Graphite Design, November 9-12, 1970, Gatlinburg, Tennessee, CONF-701105.

28. Jortner, J., "Multiaxial Behavior of ATJ-S Graphite," Technical Report AFML-TR-71-160, July 1971.

29. Jortner, J., "Multiaxial Response of ATJ-Graphite," Technical Report Afml-TR-71-253, December 1971.

30. Jortner, J., "Multiaxial Response of ATJ-S Graphite," Technical Report AFML-TR-73-170, October 1973.

31. Mair, W.M., "Fracture Criteria for Cast Iron Under Biaxial Stress," Journal of Strain Analysis, Vol. 3, No. 4, April 1968, pp. 254-263.

32. Merkle, J.G., "An Ellipsoidal Yield Function for Materials that can Both Dilate and Compact Inelastically," Nuclear Engineering and Design, 12, 1970, pp. 425-451.

33. Nadai, A., Theory of Flow and Fracture of Solids, 2nd Edition, McGraw-Hill Book Company, New York, 1950.

34. Nightingale, R.E., ed., Nuclear Graphite, Academic Press, 1962.

35. Peng, S.D., "Stresses Within Elastic Circular Cylinders Loaded Uniaxially and Triaxially," Int. J. Rock Mech. Min. Sci., Vol. 8, 1971, pp. 399-432.

36. Priddy, T.G., "A Fracture Theory for Brittle Anisotropic Materials," Journal of Engineering Materials and Technology, April 1974, pp. 91-96.

37. Rowley, J.C., "Description of Design Requirements for Graphite Components," Proceedings of the Conference on Continuum Aspects of Graphite Design, November 9-12, 1970, Gatlinburg, Tennessee, CONF-701105.

38. Sedlacek, R. and F.A. Holden, "Methods of Tensile Testing of Brittle Materials," Review of Scientific Instruments, Vol. 3, No. 3, pp. 289-300, 1962.

39. Swartz, S.E., K.K. Hu, C.M. Huang, and G.L. Jones, "An Apparatus for Tensile Testing of Concrete," Experimental Mechanics, March 1979, pp. 109-111.

40. Tang, P.Y. "A Recommendation of a Triaxial Failure Theory for Graphite," U.S. Department of Commerce, Department of Commerce, Department of Energy, No. GA-A1533 UC-77, May 1979.

41. Taylor, R., R.G. Brown, K. Gilchrist, E. Hall, A.T. Hodds, B.T. Kelly, and F. Morris, "The Mechanical Properties of Reactor Graphite," Carbon, Vol. 5, 1967, pp. 519-531.

42. Timoshenko S., Theory of Elastic Stability, 1st Edition, McGraw-Hill Book Company, New York, 1936, pp. 439-460.

43. Tsai, S.W. and F.M. Wu, "A General Theory of Strength for Anisotropic Materials," Journal of Composite Materials, Vol. 5, January 1971, pp. 58-80.

44. Union Carbide Corporation, The Industrial Graphite Engineering Handbook, Union Carbide Corporation, New York, 1970, pp. 5A.10

45. Weng, T., "Biaxial Fracture Strength and Mechanical Properties of Graphite-Base Refractory Composites," AIAA Journal, Vol. 7, No. 5, May 1969, pp. 851-858.

46. Weng, T., "Room Temperature Fracture Behavior of Polycrystalline Graphites Under Torsional and Biaxial Stesses," Paper No. MI 60, Presented at Eighth Biennial Conference on Carbon, Buffalo, N.Y., June 19-23, 1967.

47. Weng, T. "Stress-Strain Properties of Grade ATJ Graphite Under Combined Stresses," Proceedings of the Conference on Continuum Aspects of Graphite Design, November 9-12, 1970, Gatlinburg, Tennessee, CONF-701105, NTIS. U.S. Department of Commerce, pp. 222-235.

48. Weng, T., "Structural and Physical Properties of Graphite-Zirconium Diboride-Silicon Carbide Composites," Technical Report AFML-TR-70-50, May 1970, Union Carbide Corporation, Carbon Products Division, pp. 31-33.

VITA

H. Alan Hackerott

Candidate for the Degree of

Master of Science

Thesis: Characterization of Multiaxial Fracture Strength of Transversely Isotropic AGOT Graphite

Major Field: Mechanical Engineering

Biographical:

Personal Data: Born Hays, Kansas, May 21, 1958; son of Harold L. and Ruth A. Hackerott.

Education: Attended Fort Hays State University, September 1976 to May 1978; received Bachelor of Science degree in Mechanical Engineering, Kansas State University, May 1980.

Professional and Honorary Organizations: American Society of Mechanical Engineers, Society of Experimental Stress Analysis, Pi Tau Sigma, Tau Beta Pi, Phi Kappa Phi, Sigma Xi, "Engineer-in-Traning" certified, June 20, 1980.

Professional Experience: Engineering Assistant in Stress Analysis, The Boeing Company, Wichita, Kansas, May through August, 1979; Nuclear Safety Analyst, Kansas Gas and Electric Company, Wichita, Kansas, August 1982 through present.

CHARACTERIZATION OF MULTIAXIAL FRACTURE STRENGTH OF TRANSVERSELY ISOTROPIC AGOT GRAPHITE

by

H. ALAN HACKEROTT

B. S., Kansas State University, 1980

AN ABSTRACT OF A MASTER'S THESIS

submitted in partial fulfillment of the

requirements for the degree

MASTER OF SCIENCE

Department of Mechanical Engineering

KANSAS STATE UNIVERSITY
Manhattan, Kansas

1982

ABSTRACT

Better knowledge of brittle transversely isotropic material properties is needed to facilitate use of impoved analytical procedures now available. Thus, the specific aims of this study were to (a) characterize fracture tests of EGCR-type grade AGOT graphite by the application of a strength tensile theory, and (b) design and fabricate a multiaxial test apparatus to improve the acceptabliity of the pressure-vessel method for the biaxial-compression test.

This multiaxial testing apparatus approximated biaxial loadings of hollow cylinders which were also specifically designed and fabricated for the purpose of obtaining true material strength. The geometry of the biaxial compression cylinders required the balancing of two conflicting requirements, namely: uniform strain field and resistance to buckling.

Uniaxial fracture tests were performed along the three orthotropic material axes. These strengths are the intercepts of the biaxial stress space axes and the strength tensor ellipsoid. The tests are used in the evaluation of the strength polynomila coefficients and indicated the degree of transverse isotropy and material stress-strain relations.

A biaxial strength tensor polynomial for a transversely isotropic material contains five components that were evaluated by the use of the uniaxial strengths and a biaxial test. In comparison with other biaxial fracture tests, results of the present investigation are extensive and consistent in the biaxial compression quadrant, and therefore imply a better material characterization. This is probably due to the geometry of the large cylinders that were intended to be more resistant to premature buckling failure than those investigated previously.